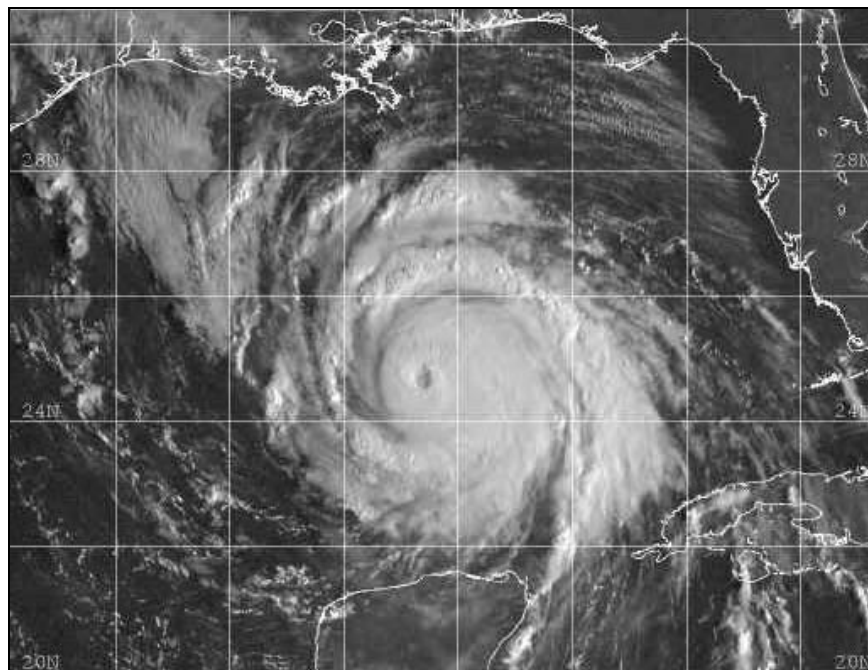


FINAL REPORT

MMS Hindcast Study of Hurricane Lili (2002) Offshore Northern Gulf of Mexico



December 2003

oceanweather inc.

5 River Road

Cos Cob, CT, USA

Tel: 203-661-3091

Fax: 203-661-6809

Email: oceanwx@oceanweather.com

Web: www.oceanweather.com

TABLE OF CONTENTS

| | |
|--|-----------|
| 1. PURPOSE | 1 |
| 2. THE HINDCAST APPROACH | 1 |
| 2.1 Introduction..... | 1 |
| 2.2 Wind Field Specification | 1 |
| 2.3 Tropical Boundary Layer Model | 2 |
| 2.4 Wave Model..... | 3 |
| 3. METEOROLOGICAL CHARACTERISTICS OF HURRICANE LILI..... | 5 |
| 3.1 Data Sources | 5 |
| 3.2 General Storm Track/Wave Characteristics..... | 5 |
| 4. HINDCAST RESULTS | 7 |
| 4.1 Wind Field | 7 |
| 4.2 Surface Waves | 8 |
| 5. VALIDATION..... | 9 |
| 5.1 NDBC Buoys..... | 9 |
| 5.2 Altimeter Measurements | 26 |
| 6. DELIVERABLES | 28 |
| References | 29 |
| | |
| APPENDIX A. Hindcast Track and Intensity of Hurricane Lili | |
| APPENDIX B. Vector Field Plots of Hindcast and Measured Winds | |
| APPENDIX C. Vector Field Plots of Hindcast and Measured Waves | |
| APPENDIX D. Fields Definitions | |

1. PURPOSE

The purpose of this study is to develop a description of the evolution and distribution of the surface wind field, wave, salinity, sea surface temperature and current field in the northern Gulf of Mexico during the approach and passage of Hurricane Lili (2002). The hindcast utilized all available public domain meteorological and oceanographic measured data, and Oceanweather's most accurate cyclone wind and wave hindcast methods. Hindcast results are validated against available measured data and an assessment of the accuracy of the hindcast provided with the results. Hindcast results will be presented in tabular, graphical and computer readable form. This narrative report includes a description of the data sources, storm evolution (track and intensity), wind and wave hindcast method and a summary of results. The ocean model hindcast methodology and results are described in a companion report.

2. THE HINDCAST APPROACH

2.1 Introduction

The hindcast of a historical storm consists of three basic steps. First, the wind field is specified in a process that requires considerable work by a meteorologist to develop required input parameters for a tropical boundary layer model. Second step is to produce kinematic analysis for use in areas in which the numerical model solution is not sufficiently accurate. Third, the resulting wind fields are applied in proven ocean wave and hydrodynamical models. In this section we give concise descriptions of each of these processes, more extensive mathematical treatments are reserved to cited references.

2.2 Wind Field Specification

The method used in this study has been applied in over three-dozen studies involving almost all basins on the globe within which tropical cyclones can occur. The method starts from raw data whenever possible and includes an intensive reanalysis of traditional cyclone parameters such as track and intensity (in terms of pressure) and then develops new estimates of the more difficult storm parameters, such as the shape of the radial pressure profile and the ambient pressure field within which the cyclone is embedded. The time histories of all of these parameters are specified within the entire period to be hindcast. Storm track and storm parameters are then used to drive a numerical primitive equation model of the cyclone boundary layer to generate a complete picture of the time-varying wind field associated with the cyclone circulation itself. That solution is then compared to time histories of accurately measured surface winds (reduced to standard height) at available measurement sites, and if necessary the storm parameters are varied and the model iterated until good agreement is obtained between the modeled wind field and the discrete high-quality wind observations available.

The resulting tropical wind field is then blended into a basin-wide field, which incorporates both atmospheric modeled winds, insitu measurements from buoys, CMAN stations, ship reports as well as satellite estimates of wind from altimeter and scatterometer instruments. Additional kinematic analysis of the tropical winds is also performed in this step. The period of Sep-28-2002 00:00 GMT to Oct-06-2002 00:00 was hindcast to allow sufficient spin-up/spin-down time for the wave and hydrodynamical models.

2.3 Tropical Boundary Layer Model

This model, first developed into a practical tool in the Ocean Data Gathering Program (ODGP) (Cardone *et al.* 1976), can provide a fairly complete description of time-space evolution of the surface winds in the boundary layer of a tropical cyclone from the simple model parameters available in historical storms. The model is an application of a theoretical model of the horizontal airflow in the boundary layer of a moving vortex. That model solves, by numerical integration, the vertically averaged equations of motion that govern a boundary layer subject to horizontal and vertical shear stresses. The equations are resolved in a Cartesian coordinate system whose origin translates at constant velocity, V_f , with the storm center of the pressure field associated with the cyclone. Variations in storm intensity and motion are represented by a series of quasi-steady state solutions. The original theoretical formulation of the model is given by Chow (1971). A similar model was described more recently in the open literature by Shapiro (1983). The version of the model applied in this study is the result of two major upgrades, one described by Cardone *et al.*, (1992) and the second by Cardone *et al.* (1994) and Thompson and Cardone (1996). The first upgrade involved mainly replacement of the empirical scaling law by a similarity boundary layer formulation to link the surface drag, surface wind and the model vertically averaged velocity components. The second upgrade added spatial resolution and generalized the pressure field specification. A more complete description of the theoretical development of the model as upgraded is given by Thompson and Cardone (1996).

The model pressure field is described as the sum of an axially symmetric part and a large-scale pressure field of constant gradient. The symmetric part is described in terms of an exponential pressure profile, which has the following parameters:

Po minimum central pressure
Pfar far-field pressure
Rp scale radius of exponential pressure profile
B profile peakedness parameter

B is an additional scaling parameter whose significance was discussed by Holland (1980). This analytical form is also used to explicitly model the storm pressure field for use in the hydrodynamic model.

The model is driven from parameters that are derived from data in historical meteorological records and the ambient pressure field. The entire wind field history is computed from

knowledge of the variation of those parameters along the storm track by computing solutions, or so-called “snapshots,” on the nested grid as often as is necessary to describe different stages of intensity, and then interpolating the entire time history from the snapshots.

The model was validated originally against winds measured in several ODGP storms. It has since been applied to nearly every recent hurricane to affect the United States offshore area, to all major storms to affect the South China Sea since 1945, and to storms affecting many other foreign basins including the Northwest Shelf of Australia, Tasman Sea of New Zealand, Bay of Bengal, Arabian Sea and Caribbean Sea. Comparisons with over-water measurements from buoys and rigs support an accuracy specification of ± 20 degrees in direction and ± 2 meters/second in wind speed (1-hour average at 10-meter elevation). Many comparisons have been published (see e.g., Ross and Cardone, 1978; Cardone and Ross, 1979; Forristall *et al.*, 1977; 1978; 1980; Cardone *et al.*, 1992, Cardone and Grant, 1994).

As presently formulated, the wind model is free of arbitrary calibration constants, which might link the model to a particular storm type or region. For example, differences in latitude are handled properly in the primitive equation formulation through the Coriolis parameter. The variations in structure between tropical storm types manifest themselves basically in the characteristics of the pressure field of the vortex itself and of the surrounding region. The interaction of a tropical cyclone and its environment, therefore, can be accounted for by a proper specification of the input parameters. The assignable parameters of the planetary boundary layer (PBL) formulation, namely planetary boundary layer depth and stability, and of the sea surface roughness formulation, can safely be taken from studies performed in the Gulf of Mexico, since tropical cyclones world-wide share a common set of thermodynamic and kinematic constraints.

2.4 Wave Model

OWI’s standard UNIWAVE high-resolution full spectral wave hindcast model was used for all wave hindcasts. UNIWAVE incorporates deep water and shallow processes and the option to use either OWI’s highly calibrated first generation source term physics (ODGP2) or third generation (3G) physics (OWI3G/DIA2). Extensive validations of OWI’s wave models in long-term hindcast studies are given recently by Swail and Cox (2000) and Cox and Swail (2001). Details on the 3rd generation physics applied in UNIWAVE can be found in Khandekar *et al.* (1994).

The MMSLILI implementation of the UNIWAVE model was applied in the Hurricane Lili hindcast using 3G physics. The grid domain is from 18N to 31N and 98W to 80W with grid spacing of .05 degree (Figure 1). Bathymetry for the model was obtained from the GEBCO (General Bathymetric Chart of the Oceans) Centenary Edition CD-ROM 1-minute dataset.

Hindcast of Hurricane Lili (2002)

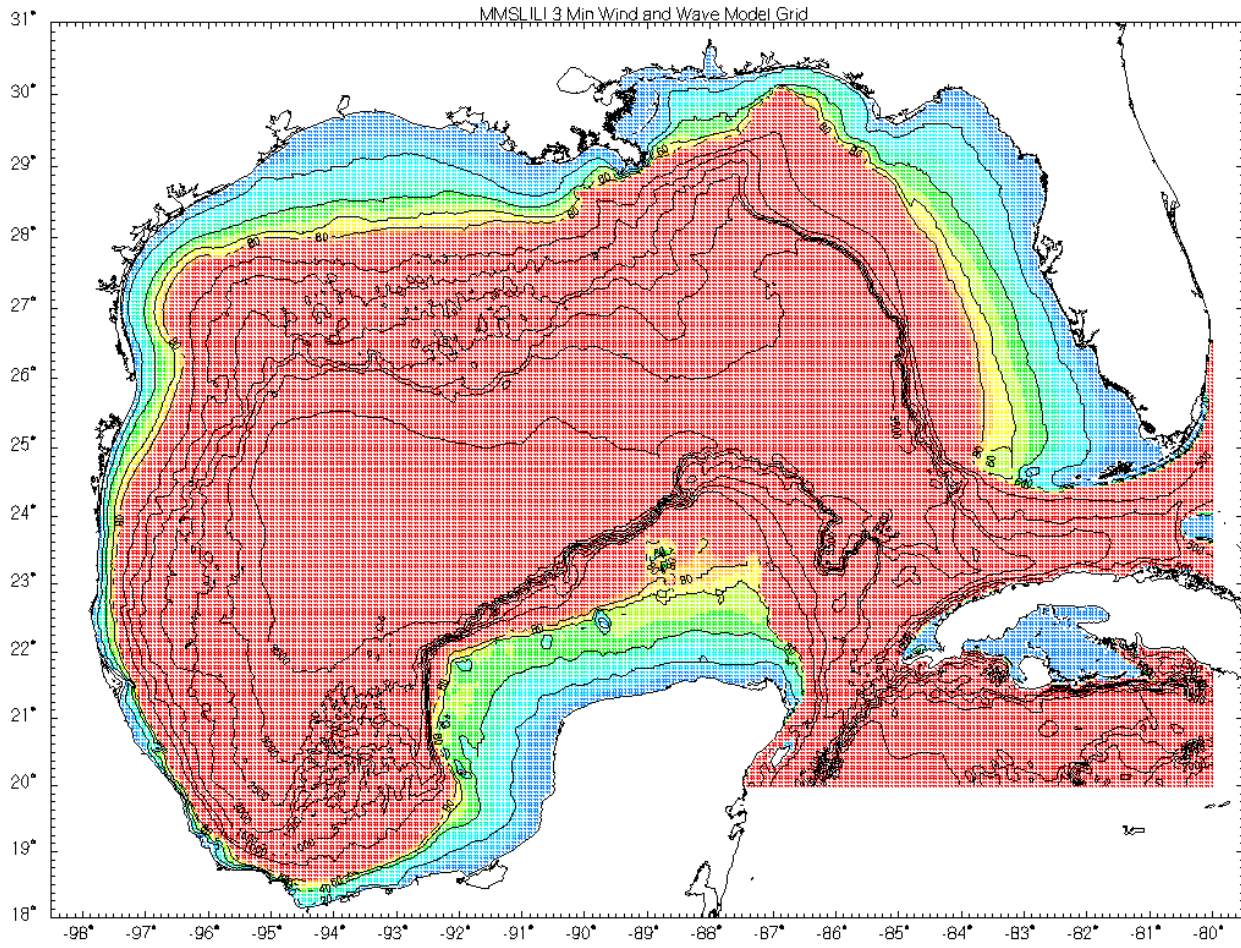


Figure 1 MMSLili 3-Minute hindcast model grid

3. METEOROLOGICAL CHARACTERISTICS OF HURRICANE LILI

3.1 Data Sources

Our analysis referred to the following data:

- Aircraft reconnaissance of Hurricane Lili obtained from NOAA and U.S. Air Force hurricane hunter aircraft, including vortex messages as well as continuous flight level wind speed, direction, D-Value, air temperature.
- Gridded and image fields of marine surface wind composites from the Hurricane Research Division HWnd re-analysis of Lili
- Synoptic observations from NOAA buoy and C-MAN stations
- Synoptic observations from coastal and land stations obtained from the GTS (Global Transmission System) in real time
- NOAA NHC/TPC advisories including intensity and position at 3-hourly intervals.
- NHC/TPC best track data
- NHC/TPC Tropical Storm Report
- Composite NWS radar imagery
- Loops of NOAA GOES visual, infrared and water vapor imagery
- NWS synoptic weather analysis charts
- NCEP model wind fields
- QUIKSCAT scatterometer winds
- TOPEX altimeter winds and waves
- ERS-2 altimeter winds and waves

3.2 General Storm Track/Wave Characteristics

The full track of Hurricane Lili is shown in Figure 2 and a more detailed track in the Northern Gulf of Mexico is shown in Figure 3 along with the locations of NDBC buoy stations. The path of Lili passed very close to NDBC buoys 42001 (Mid Gulf buoy located at 25°55'12"N 89°40'48"W in 3,246 meters of water) and 42041 (North Mid Gulf buoy located at 27°30'00" N 90°30'00"W in 1,435.6 meters of water). 42001 is a 10-meter discuss buoy with wind measurements at 10 meters above the sea surface while 42041 is a smaller 3-meter discuss which measures winds at 5 meters above the sea surface. 42001 measured an 11.2-meter peak significant wave height at 02/21 GMT with adjusted wind speed of 47.2 m/s one hour later

Hindcast of Hurricane Lili (2002)

(unsmoothed). 42041 measured a 12.3-meter peak significant wave height 03/03 GMT with adjusted wind speed of 31.9 m/s. This wave peak, reported in real time, was later dropped in the quality controlled buoy files available from NDBC leaving the 03/01 GMT report of 10.1 meters as the measured peak wave at 42041.

The Tropical Prediction Center storm report for Lili is available at <http://www.nhc.noaa.gov/2002atlan.shtml>. A copy of this report is available on the delivery volume as well.

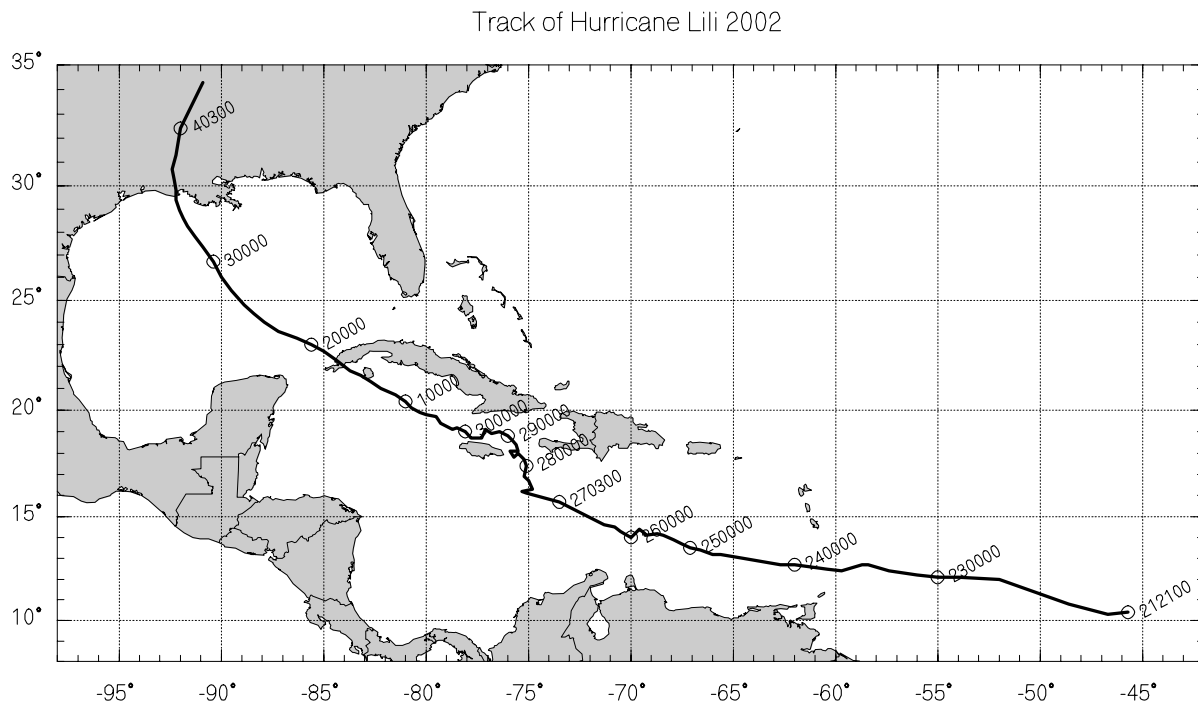


Figure 2 Track of Hurricane Lili 2002 (time GMT in DDHHMM format)

Hindcast of Hurricane Lili (2002)

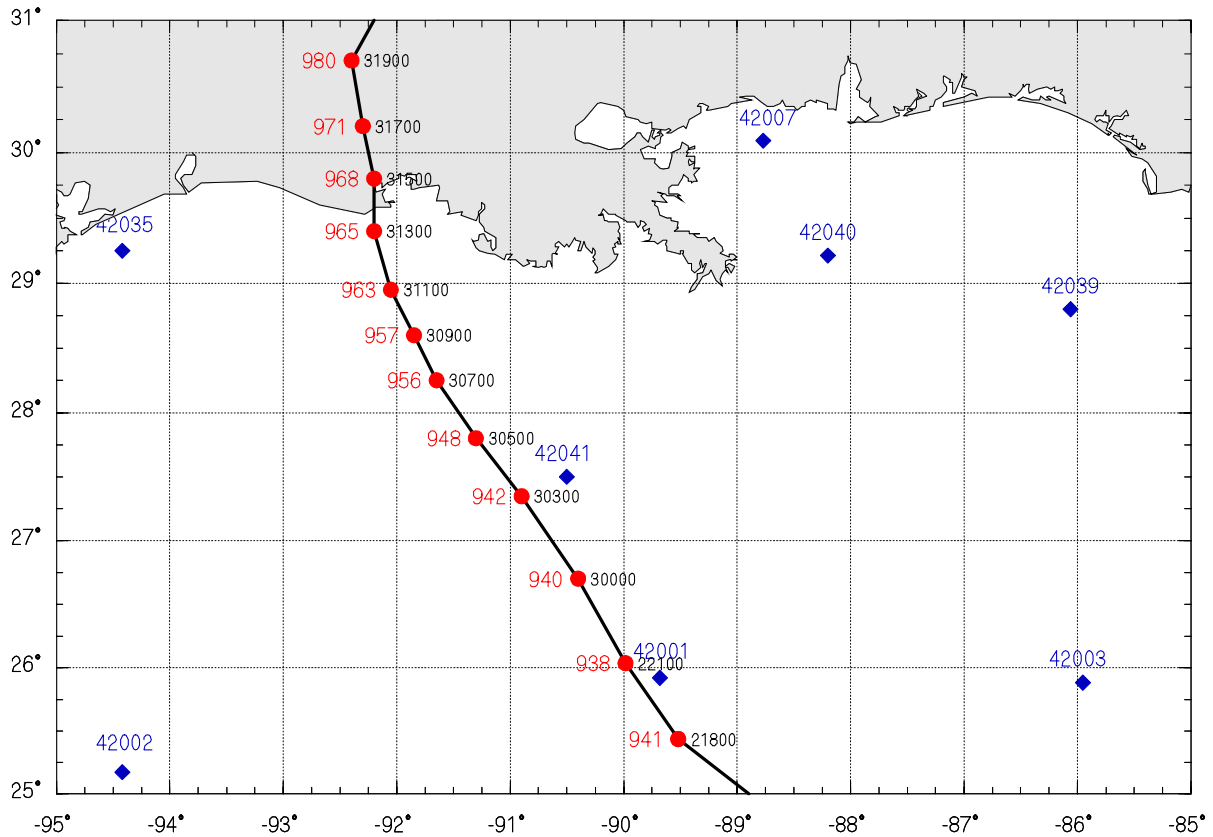


Figure 3 Track of Lili in Northern Gulf with fix time (black, GMT, DDHHMM format), central pressure (red, mb) and NDBC buoy locations (blue).

4. HINDCAST RESULTS

4.1 Wind Field

In this study all winds are referred to the effective over-water 30-minute average winds at a height of 10 meters above sea level. Applying the following “gust” factors to the 30-minute average wind speed may derive wind speeds at shorter averaging intervals:

| | |
|-------------------|--------|
| 10-minute average | x 1.09 |
| 1-minute average | x 1.24 |
| 3-second gust | x 1.53 |

The maximum hindcast wind speeds in Lili are shown in Figure 4; hourly plots of wind fields are available in the Appendix.

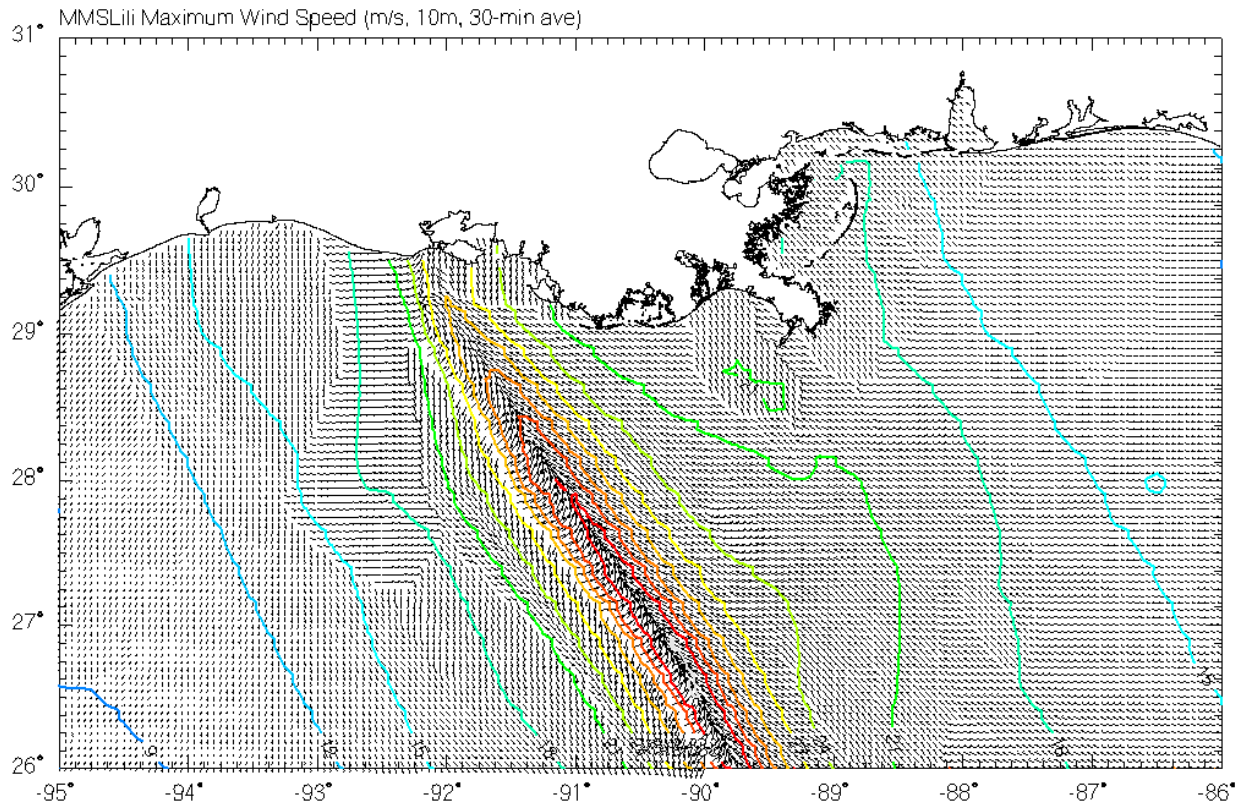


Figure 4 Maximum hindcast wind speed (m/s) during Hurricane Lili 2002

4.2 Surface Waves

The execution of the UNIWAVE hindcast model provides directly the two-dimensional wave spectrum at 15-minute intervals on the MMSLILI model grid. Integrated properties of the spectrum are calculated from the 2-D spectrum at all Northern Gulf grid points and archived as part of the hindcast run. The maximum hindcast significant wave heights in Lili are shown in Figure 5; hourly plots of wave fields are available in the Appendix.

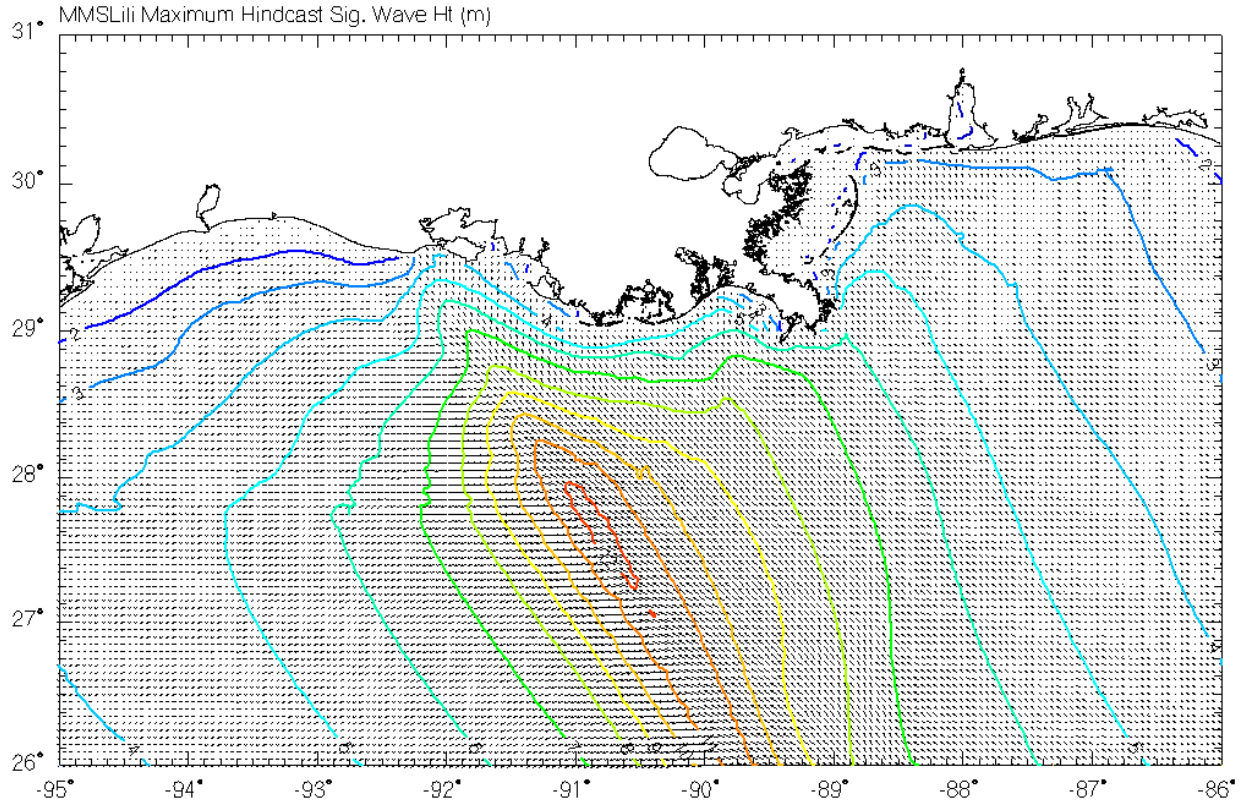


Figure 5 Maximum hindcast significant wave heights (m) during Hurricane Lili 2002

5. VALIDATION

5.1 NDBC Buoys

Validation of the hindcast was performed against all available NDBC buoys in the Gulf of Mexico as listed in Table 1. Data were obtained from quality controlled files available from the National Oceanographic Data Center and have undergone additional quality control procedure not possible in real-time. All wind speed have been adjusted for height and stability to a reference level of 10 meters and all data has been smoothed +/- 1 hour with equal weighting to

Hindcast of Hurricane Lili (2002)

reduce sampling variability. CMAN stations, which do not report waves in the Gulf, were not included in the validation dataset. Figures 8-13 show time series for each of the buoys, statistics for the hindcast are in Table 2.

Wave spectra comparisons were made from the format F291 files available from NDBC. No attempt to smooth the spectra was made. All buoys reported directional wave data with the exception of buoy 42041. Figures 13-18 show spectra comparisons just before, at, and just after the peak wave conditions at buoys 42001 and 42041.

Table 1 Validation Dataset

| <i>NDBC Measurement Locations</i> | | | | <i>Hindcast Locations</i> | | | |
|-----------------------------------|----------|-----------|--------------|---------------------------|----------|-----------|--------------|
| Location | Latitude | Longitude | Depth (m) | GridPoint | Latitude | Longitude | Depth (m) |
| 42001 | 25.92 | -89.68 | 3,246 | 39530 | 25.9 | -89.7 | 3,212 |
| 42002 | 25.17 | -94.42 | 3,200 | 34589 | 25.15 | -94.4 | 3,617 |
| 42003 | 25.88 | -85.95 | 3,164 | 39605 | 25.9 | -85.95 | 3,216 |
| 42007 | 30.09 | -88.77 | 13.4 | 60633 | 30.1 | -88.75 | 8 |
| 42019 | 27.92 | -95.36 | 82.3 | 51358 | 27.9 | -95.35 | 87 |
| 42020 | 26.95 | -96.7 | 78.6 | 45790 | 26.95 | -96.7 | 83 |
| 42035 | 29.25 | -94.41 | 15.9 | 58344 | 29.25 | -94.4 | 9 |
| 42036 | 28.51 | -84.51 | 53.0 | 54874 | 28.5 | -84.5 | 51 |
| 42039 | 28.8 | -86.06 | 283.5 | 56409 | 28.8 | -86.05 | 294 |
| 42040 | 29.21 | -88.2 | 237.7 | 58235 | 29.2 | -88.2 | 247 |
| 42041 | 27.5 | -90.5 | 1,435.6 | 49164 | 27.5 | -90.5 | 1045 |

Hindcast of Hurricane Lili (2002)

Table 2 Comparison statistics for time period Oct-01-2002 to Oct-04-2002 in the Gulf of Mexico during passage of Hurricane Lili.

| | <i>Station</i> | <i>#</i> | <i>Mean Meas</i> | <i>Mean Hind</i> | <i>(H-M)</i> | <i>RMS Error</i> | <i>Std Dev</i> | <i>Scatter Index</i> | <i>Corr Coeff</i> |
|-----------------|----------------|----------|------------------|------------------|--------------|------------------|----------------|----------------------|-------------------|
| Wind Spd. (m/s) | 42001 | 85 | 10.72 | 10.77 | 0.05 | 0.80 | 0.80 | 0.07 | 1.00 |
| Wind Dir. (deg) | 42001 | 85 | 114.63 | 114.01 | -1.38 | N/A | 10.91 | 0.03 | N/A |
| Sig Wave Ht (m) | 42001 | 85 | 2.58 | 2.69 | 0.11 | 0.41 | 0.40 | 0.15 | 0.98 |
| Wave Period (s) | 42001 | 85 | 5.46 | 5.56 | 0.10 | 0.41 | 0.40 | 0.07 | 0.96 |
| Wave Dir (deg) | 42001 | 85 | 93.28 | 119.28 | -22.17 | N/A | 54.78 | 0.15 | N/A |
| Wind Spd. (m/s) | 42002 | 85 | 5.52 | 5.73 | 0.21 | 0.63 | 0.59 | 0.11 | 0.96 |
| Wind Dir. (deg) | 42002 | 85 | 72.11 | 67.77 | 0.33 | N/A | 9.06 | 0.03 | N/A |
| Sig Wave Ht (m) | 42002 | 85 | 1.47 | 1.52 | 0.05 | 0.29 | 0.28 | 0.19 | 0.96 |
| Wave Period (s) | 42002 | 85 | 6.02 | 5.17 | -0.86 | 1.00 | 0.51 | 0.08 | 0.96 |
| Wave Dir (deg) | 42002 | 85 | 88.10 | 69.90 | -17.97 | N/A | 15.12 | 0.04 | N/A |
| Wind Spd. (m/s) | 42003 | 85 | 8.72 | 8.96 | 0.24 | 0.64 | 0.60 | 0.07 | 0.99 |
| Wind Dir. (deg) | 42003 | 85 | 107.13 | 106.30 | -0.83 | N/A | 7.55 | 0.02 | N/A |
| Sig Wave Ht (m) | 42003 | 85 | 2.57 | 2.20 | -0.38 | 0.49 | 0.32 | 0.12 | 0.99 |
| Wave Period (s) | 42003 | 85 | 6.36 | 5.38 | -0.98 | 1.08 | 0.45 | 0.07 | 0.91 |
| Wave Dir (deg) | 42003 | 85 | 142.88 | 121.49 | -27.93 | N/A | 34.12 | 0.09 | N/A |
| Wind Spd. (m/s) | 42007 | 85 | 11.54 | 11.50 | -0.04 | 0.81 | 0.80 | 0.07 | 0.98 |
| Wind Dir. (deg) | 42007 | 85 | 103.76 | 104.65 | 0.79 | N/A | 4.41 | 0.01 | N/A |
| Sig Wave Ht (m) | 42007 | 85 | 1.80 | 1.46 | -0.34 | 0.51 | 0.38 | 0.21 | 0.98 |
| Wave Period (s) | 42007 | 85 | 5.18 | 4.46 | -0.72 | 0.92 | 0.58 | 0.11 | 0.97 |
| Wave Dir (deg) | 42007 | 85 | 128.14 | 117.37 | -10.97 | N/A | 9.29 | 0.03 | N/A |
| Wind Spd. (m/s) | 42019 | 85 | 6.42 | 6.30 | -0.12 | 0.67 | 0.66 | 0.10 | 0.83 |
| Wind Dir. (deg) | 42019 | 85 | 101.89 | 101.07 | -1.53 | N/A | 5.80 | 0.02 | N/A |
| Sig Wave Ht (m) | 42019 | 85 | 1.40 | 1.32 | -0.07 | 0.36 | 0.35 | 0.25 | 0.95 |
| Wave Period (s) | 42019 | 85 | 5.26 | 4.65 | -0.60 | 0.94 | 0.73 | 0.14 | 0.96 |
| Wave Dir (deg) | 42019 | 85 | 114.05 | 100.47 | -14.35 | N/A | 23.34 | 0.06 | N/A |

Hindcast of Hurricane Lili (2002)

| | <i>Station</i> | <i>#</i> | <i>Mean Meas</i> | <i>Mean Hind</i> | <i>(H-M)</i> | <i>RMS Error</i> | <i>Std Dev</i> | <i>Scatter Index</i> | <i>Corr Coeff</i> |
|-----------------|----------------|----------|----------------------|----------------------|--------------|----------------------|--------------------|--------------------------|-----------------------|
| Wind Spd. (m/s) | 42020 | 85 | 5.37 | 5.67 | 0.30 | 1.30 | 1.27 | 0.24 | 0.84 |
| Wind Dir. (deg) | 42020 | 85 | 109.20 | 110.34 | -0.44 | N/A | 18.11 | 0.05 | N/A |
| Sig Wave Ht (m) | 42020 | 85 | 1.31 | 1.31 | 0.00 | 0.32 | 0.32 | 0.24 | 0.95 |
| Wave Period (s) | 42020 | 85 | 5.33 | 4.98 | -0.35 | 0.71 | 0.61 | 0.11 | 0.94 |
| Wave Dir (deg) | 42020 | 85 | 112.59 | 98.89 | -13.66 | N/A | 14.51 | 0.04 | N/A |
| Wind Spd. (m/s) | 42035 | 85 | 7.35 | 7.57 | 0.22 | 1.59 | 1.58 | 0.21 | 0.80 |
| Wind Dir. (deg) | 42035 | 85 | 90.77 | 87.66 | 0.09 | N/A | 6.61 | 0.02 | N/A |
| Sig Wave Ht (m) | 42035 | 85 | 1.08 | 0.86 | -0.22 | 0.37 | 0.31 | 0.28 | 0.89 |
| Wave Period (s) | 42035 | 85 | 4.37 | 3.85 | -0.52 | 0.64 | 0.38 | 0.09 | 0.93 |
| Wave Dir (deg) | 42035 | 85 | 153.54 | 110.96 | -29.52 | N/A | 26.75 | 0.07 | N/A |
| Wind Spd. (m/s) | 42036 | 85 | 8.41 | 8.42 | 0.01 | 0.78 | 0.78 | 0.09 | 0.91 |
| Wind Dir. (deg) | 42036 | 85 | 93.53 | 92.43 | -0.92 | N/A | 5.77 | 0.02 | N/A |
| Sig Wave Ht (m) | 42036 | 85 | 1.63 | 1.42 | -0.21 | 0.33 | 0.25 | 0.15 | 0.80 |
| Wave Period (s) | 42036 | 85 | 5.01 | 4.57 | -0.44 | 0.62 | 0.43 | 0.09 | 0.68 |
| Wave Dir (deg) | 42036 | 85 | 133.13 | 112.91 | -24.02 | N/A | 25.62 | 0.07 | N/A |
| Wind Spd. (m/s) | 42039 | 85 | 9.54 | 9.54 | 0.00 | 0.42 | 0.42 | 0.04 | 0.97 |
| Wind Dir. (deg) | 42039 | 85 | 95.39 | 97.71 | 2.37 | N/A | 4.80 | 0.01 | N/A |
| Sig Wave Ht (m) | 42039 | 85 | 2.07 | 1.83 | -0.24 | 0.31 | 0.20 | 0.10 | 0.96 |
| Wave Period (s) | 42039 | 85 | 5.41 | 4.88 | -0.53 | 0.59 | 0.25 | 0.05 | 0.93 |
| Wave Dir (deg) | 42039 | 85 | 137.38 | 113.01 | -26.91 | N/A | 18.76 | 0.05 | N/A |
| Wind Spd. (m/s) | 42040 | 85 | 10.30 | 10.40 | 0.11 | 0.58 | 0.57 | 0.06 | 0.98 |
| Wind Dir. (deg) | 42040 | 85 | 105.72 | 107.73 | 1.84 | N/A | 4.10 | 0.01 | N/A |
| Sig Wave Ht (m) | 42040 | 85 | 2.43 | 2.38 | -0.05 | 0.30 | 0.30 | 0.12 | 0.98 |
| Wave Period (s) | 42040 | 85 | 5.60 | 5.28 | -0.32 | 0.49 | 0.37 | 0.07 | 0.96 |
| Wave Dir (deg) | 42040 | 85 | 137.50 | 118.19 | -18.69 | N/A | 15.08 | 0.04 | N/A |
| Wind Spd. (m/s) | 42041 | 85 | 11.46 | 11.63 | 0.17 | 0.76 | 0.74 | 0.06 | 0.99 |
| Wind Dir. (deg) | 42041 | 85 | 106.84 | 108.89 | 0.58 | N/A | 8.72 | 0.02 | N/A |

Hindcast of Hurricane Lili (2002)

| | <i>Station</i> | <i>#</i> | <i>Mean</i> <i>Meas</i> | <i>Mean</i> <i>Hind</i> | <i>(H-M)</i> | <i>RMS</i> <i>Error</i> | <i>Std</i> <i>Dev</i> | <i>Scatter</i> <i>Index</i> | <i>Corr</i> <i>Coeff</i> |
|-----------------|----------------|----------|----------------------------|----------------------------|--------------|----------------------------|--------------------------|--------------------------------|-----------------------------|
| Sig Wave Ht (m) | 42041 | 83 | 2.91 | 2.76 | -0.15 | 0.43 | 0.40 | 0.14 | 0.98 |
| Wave Period (s) | 42041 | 83 | 5.72 | 5.42 | -0.30 | 0.52 | 0.42 | 0.07 | 0.98 |

Hindcast of Hurricane Lili (2002)

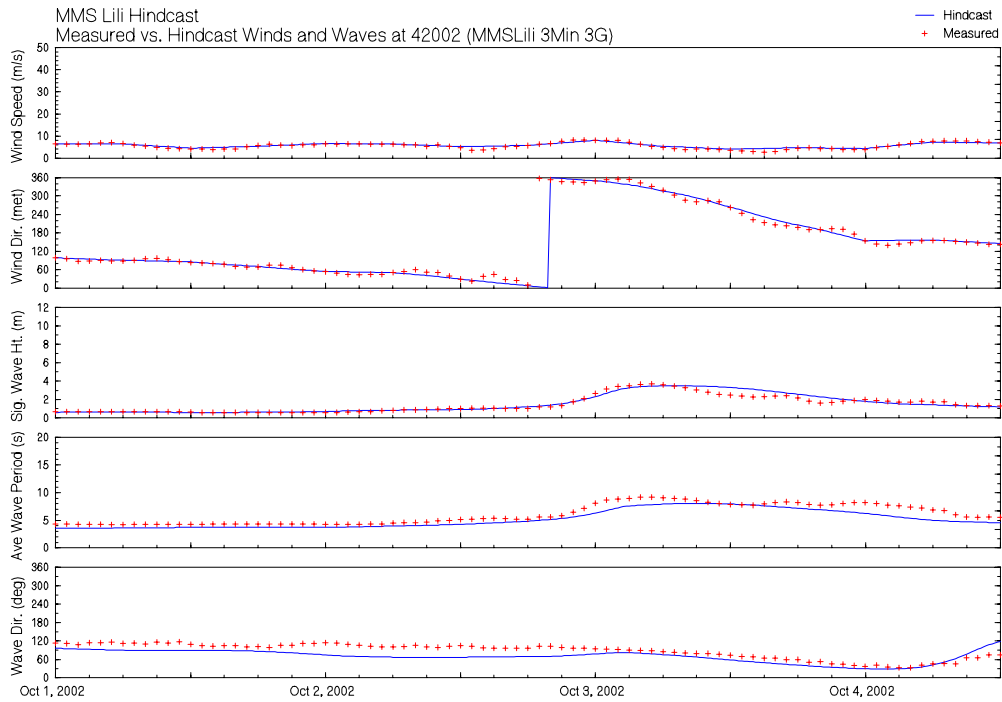
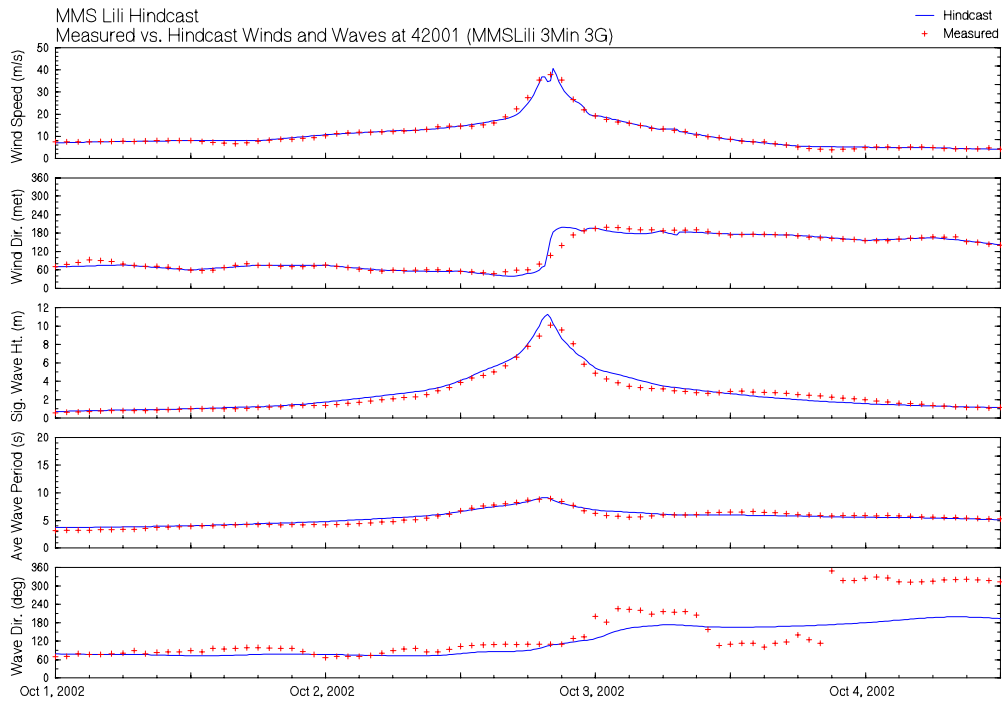


Figure 6 Timeseries comparison at Buoy 42001 (top) and 42002 (bottom)

Hindcast of Hurricane Lili (2002)

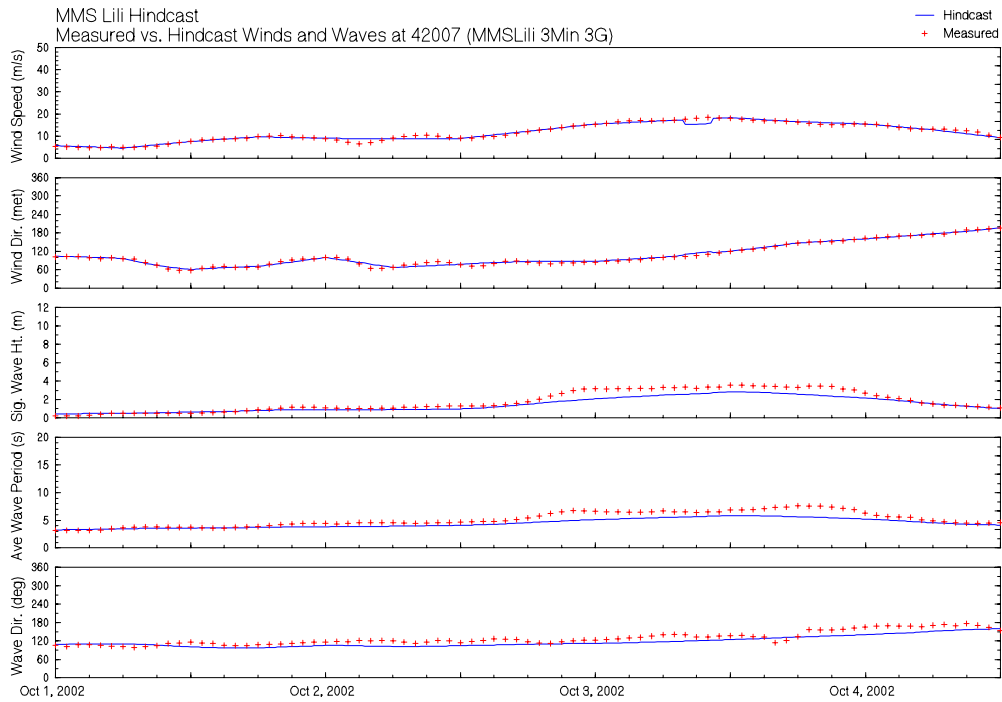
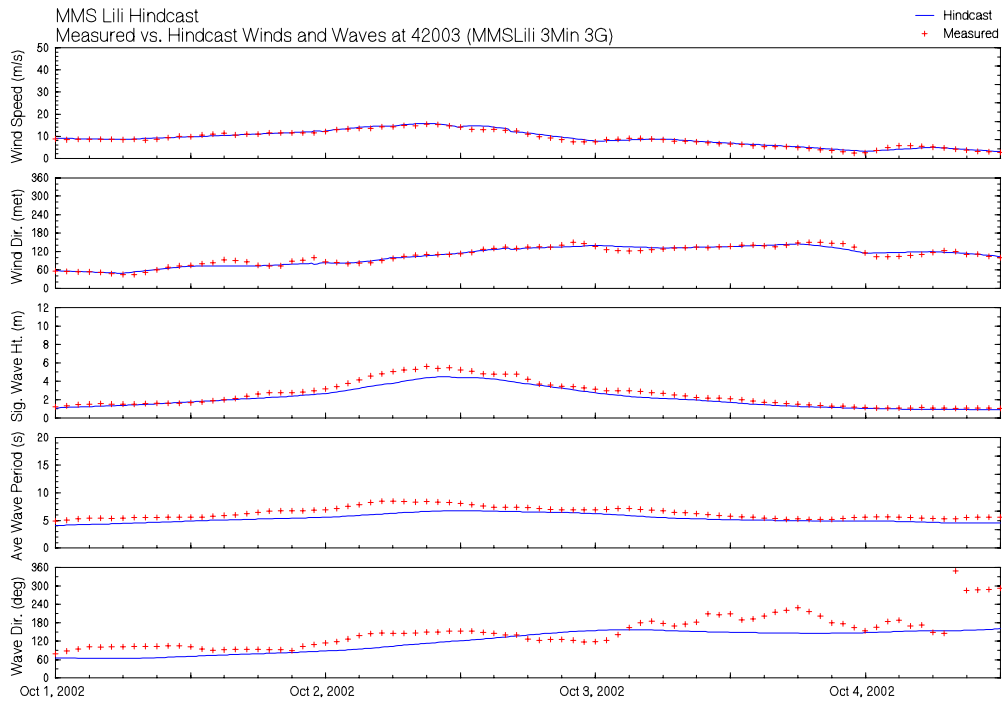


Figure 7 Timeseries comparison at Buoy 42003 (top) and 42007 (bottom)

Hindcast of Hurricane Lili (2002)

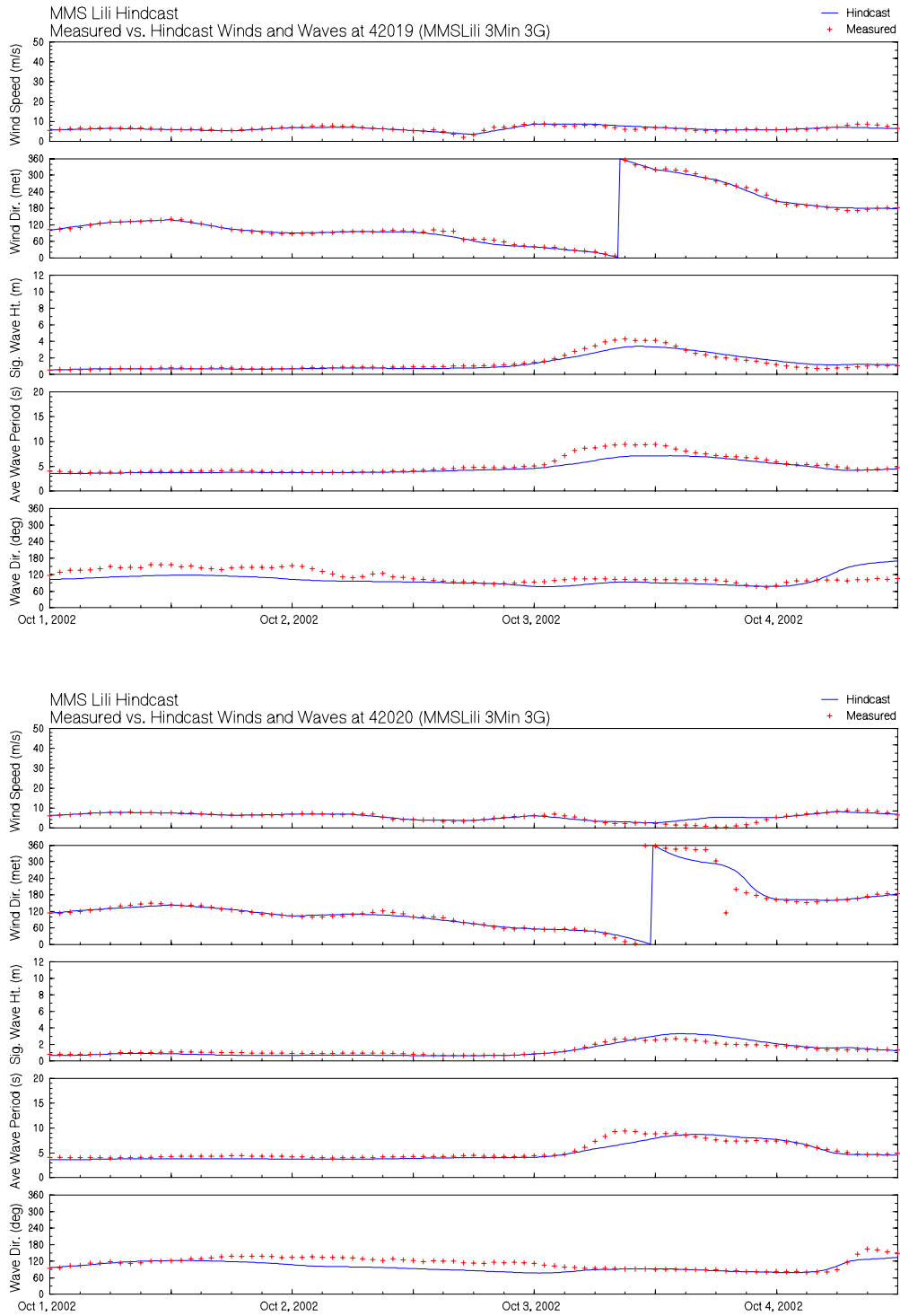


Figure 8 Timeseries comparison at Buoy 42019 (top) and 42020 (bottom)

Hindcast of Hurricane Lili (2002)

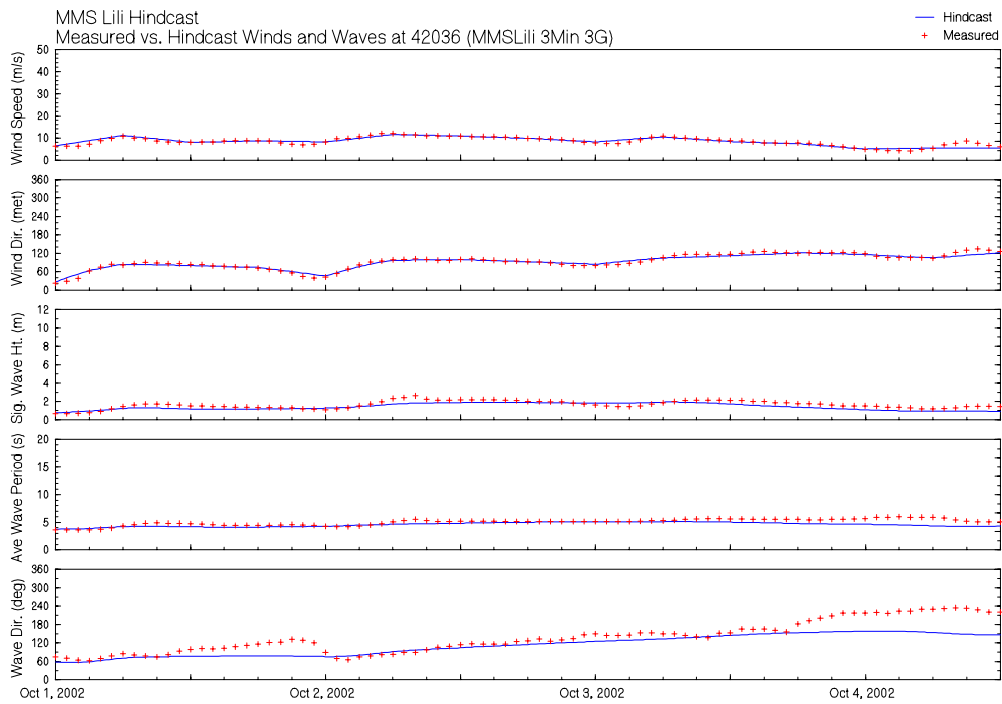
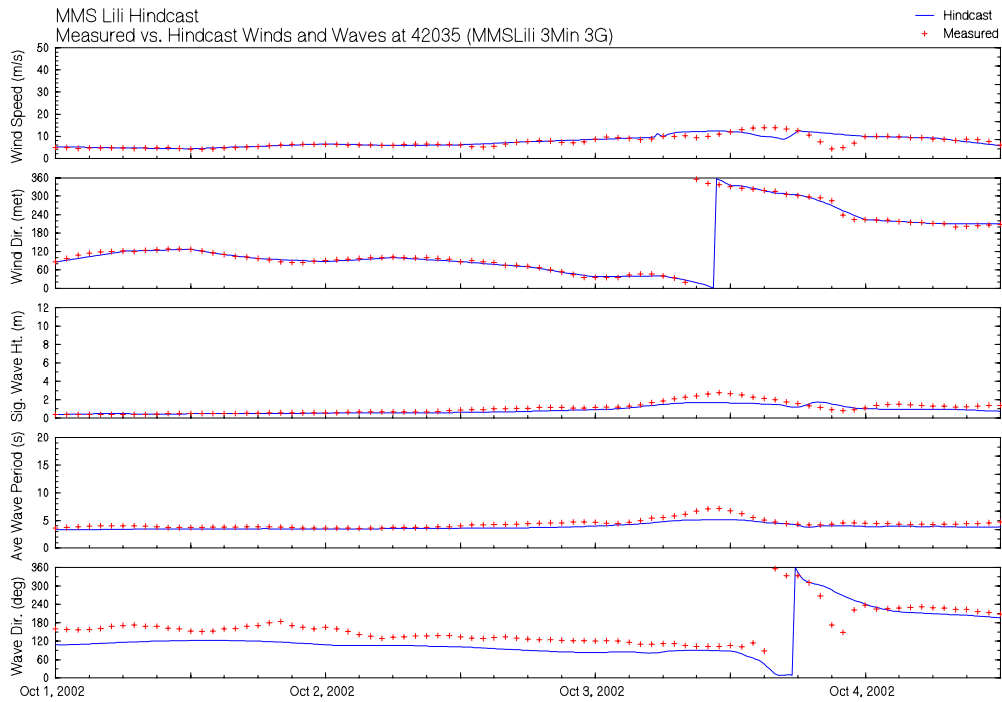


Figure 9 Timeseries comparison at Buoy 42035 (top) and 42036 (bottom)

Hindcast of Hurricane Lili (2002)

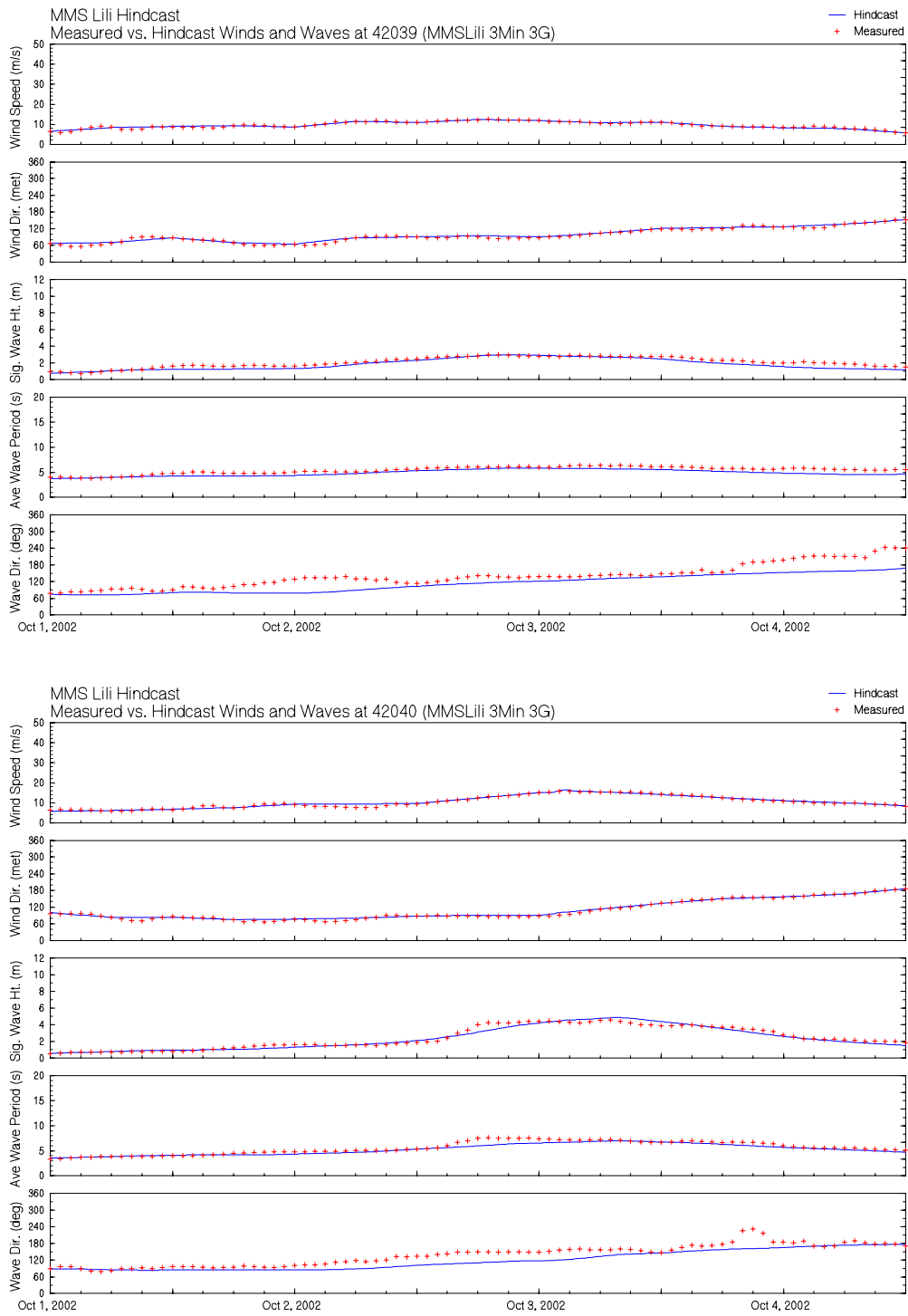


Figure 10 Timeseries comparison at Buoy 42039 (above) and 42040 (below)

Hindcast of Hurricane Lili (2002)

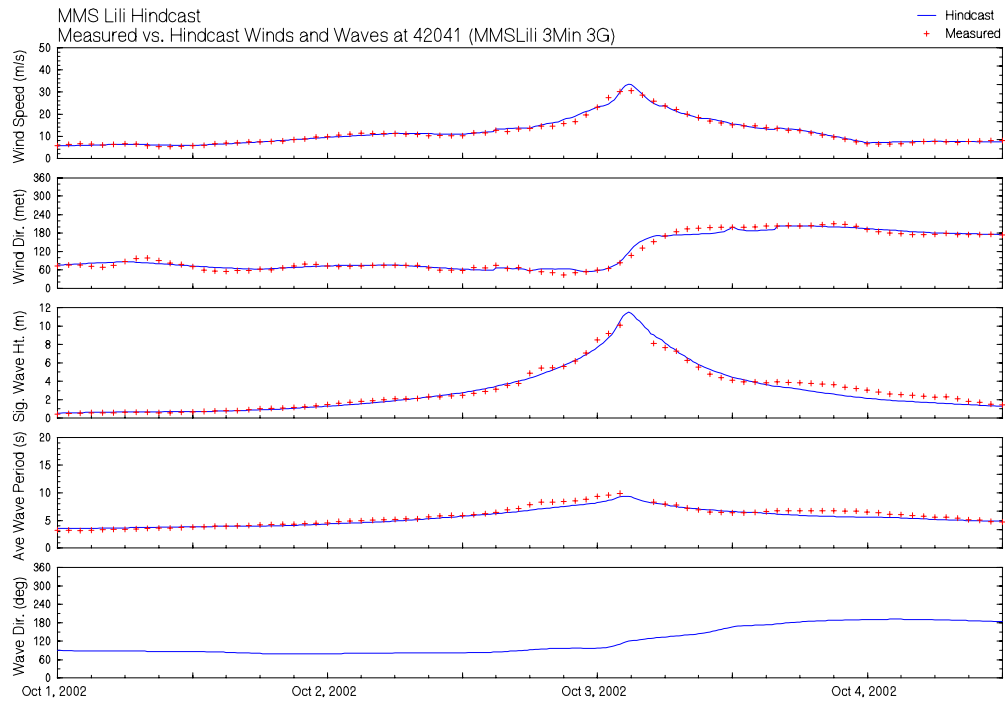


Figure 11 Timeseries comparison at Buoy 42041

Hindcast of Hurricane Lili (2002)

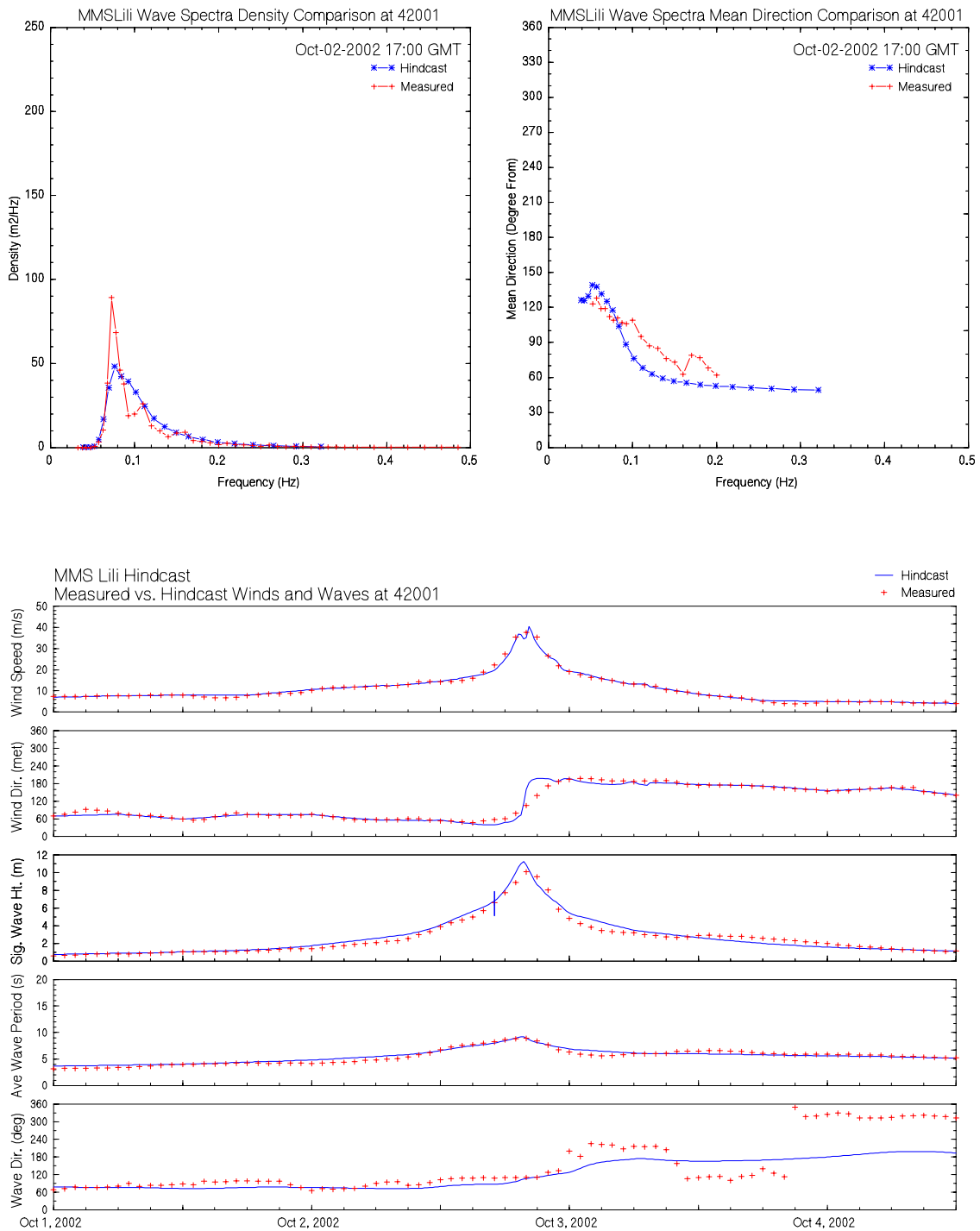


Figure 12 Wave spectra comparison at Buoy 42001 on Oct-03 17:00 GMT (3 hours before peak)

Hindcast of Hurricane Lili (2002)

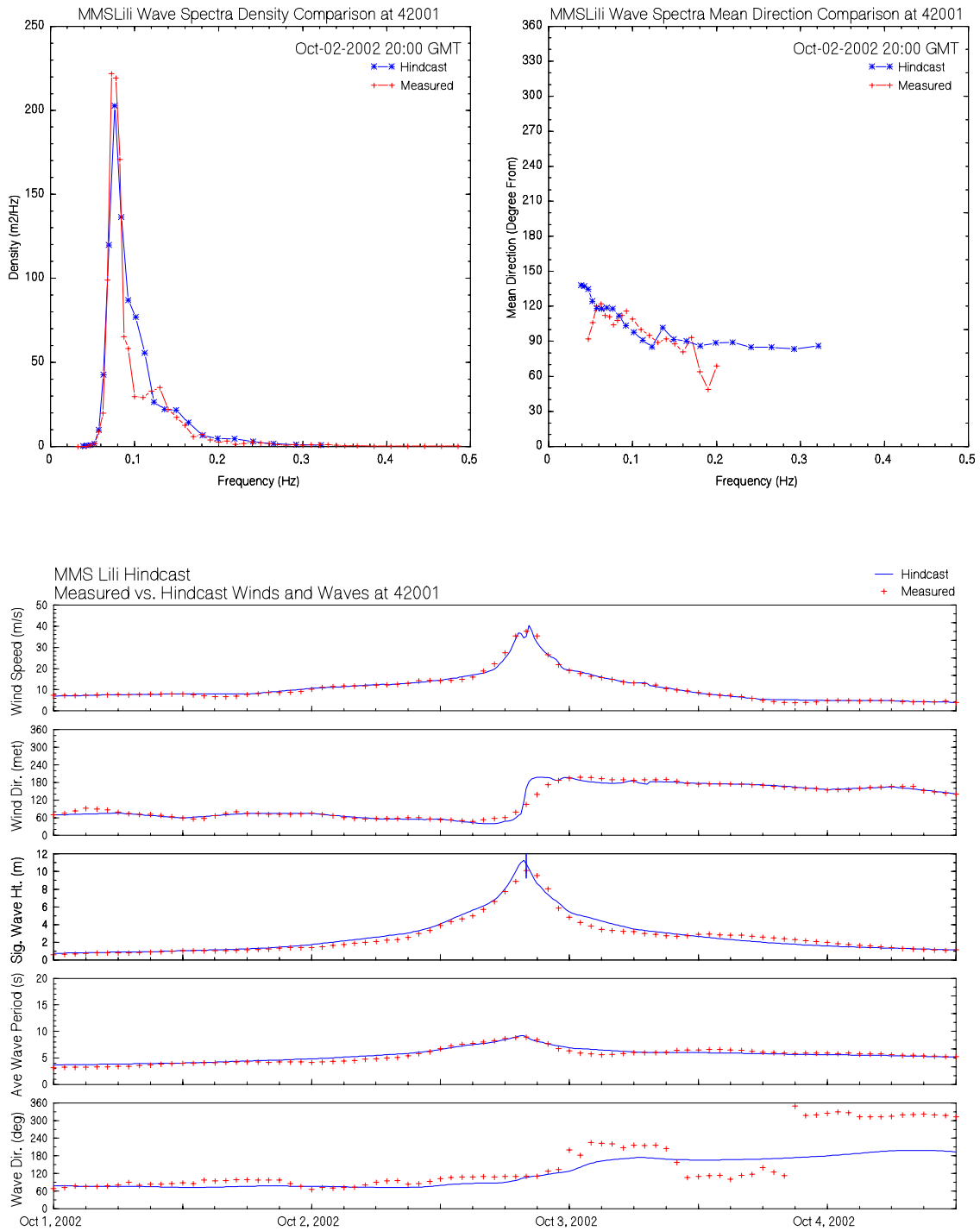


Figure 13 Wave spectra comparison at Buoy 42001 on Oct-03 20:00 GMT (wave peak)

Hindcast of Hurricane Lili (2002)

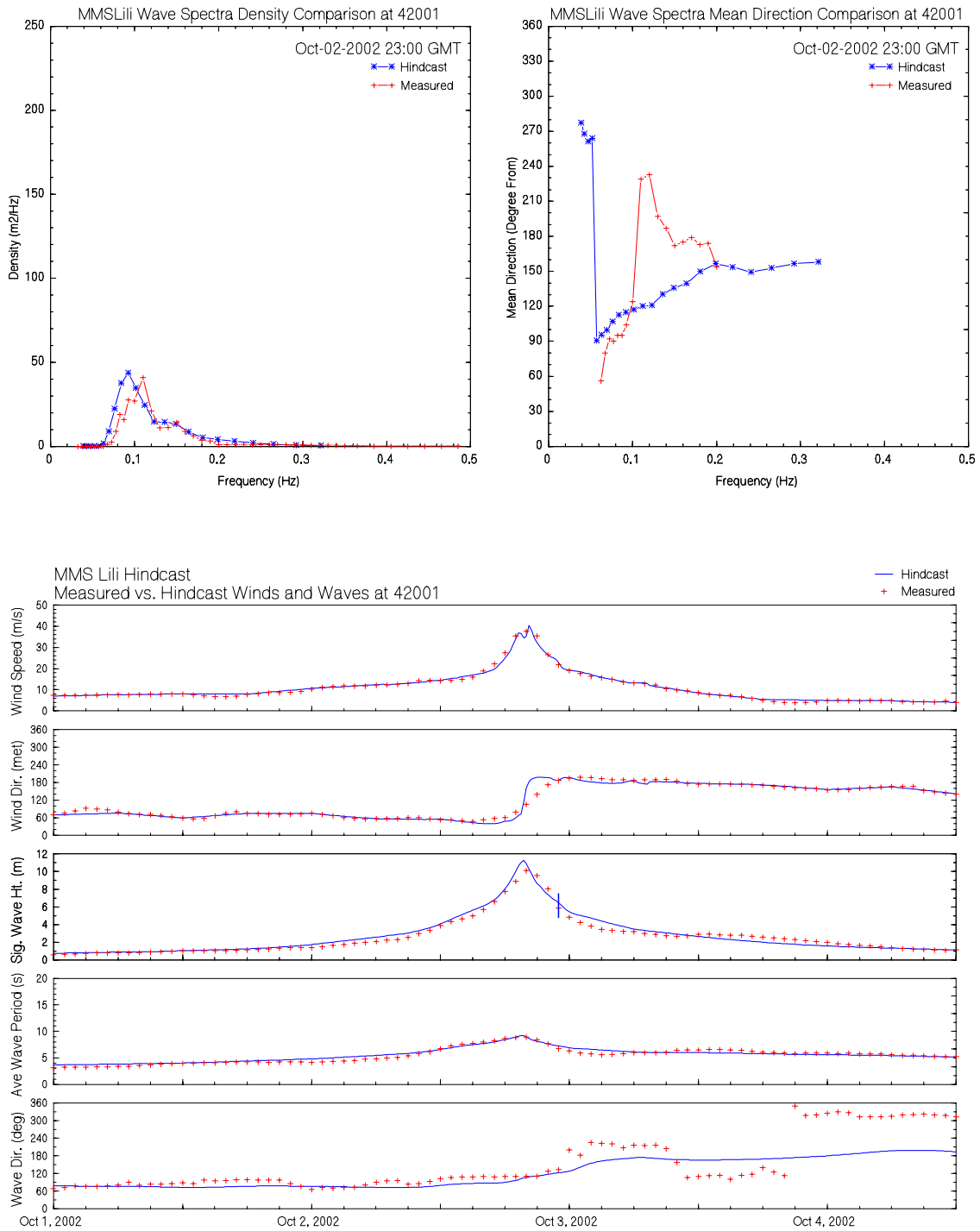


Figure 14 Wave spectra comparison at Buoy 42001 on Oct-03 23:00 GMT (3 hours after peak)

Hindcast of Hurricane Lili (2002)

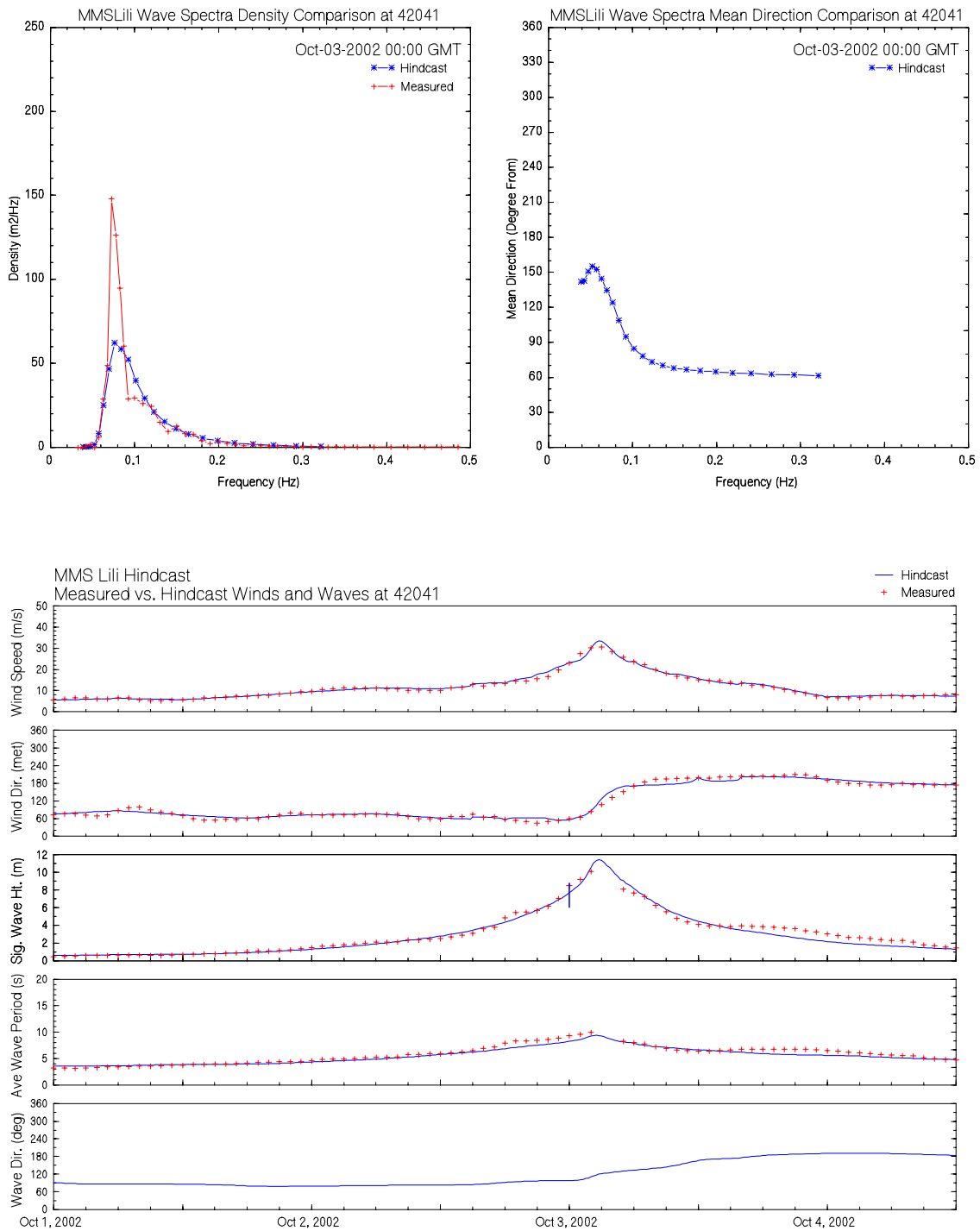


Figure 15 Wave spectra comparison at Buoy 42041 on Oct-03 00:00 GMT (3 hours before peak)

Hindcast of Hurricane Lili (2002)

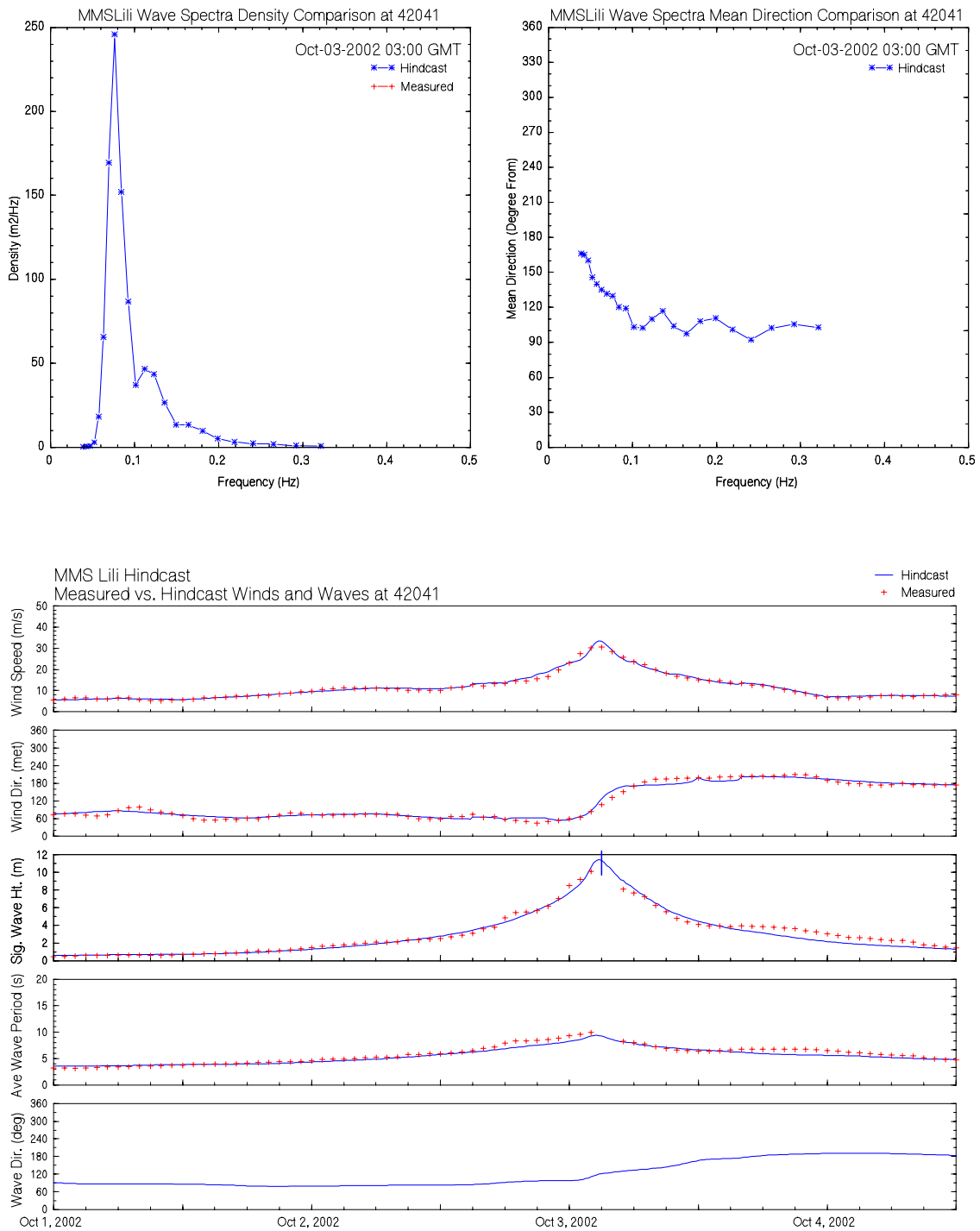


Figure 16 Wave spectra comparison at Buoy 42041 on Oct-03 03:00 GMT (wave peak)

Hindcast of Hurricane Lili (2002)

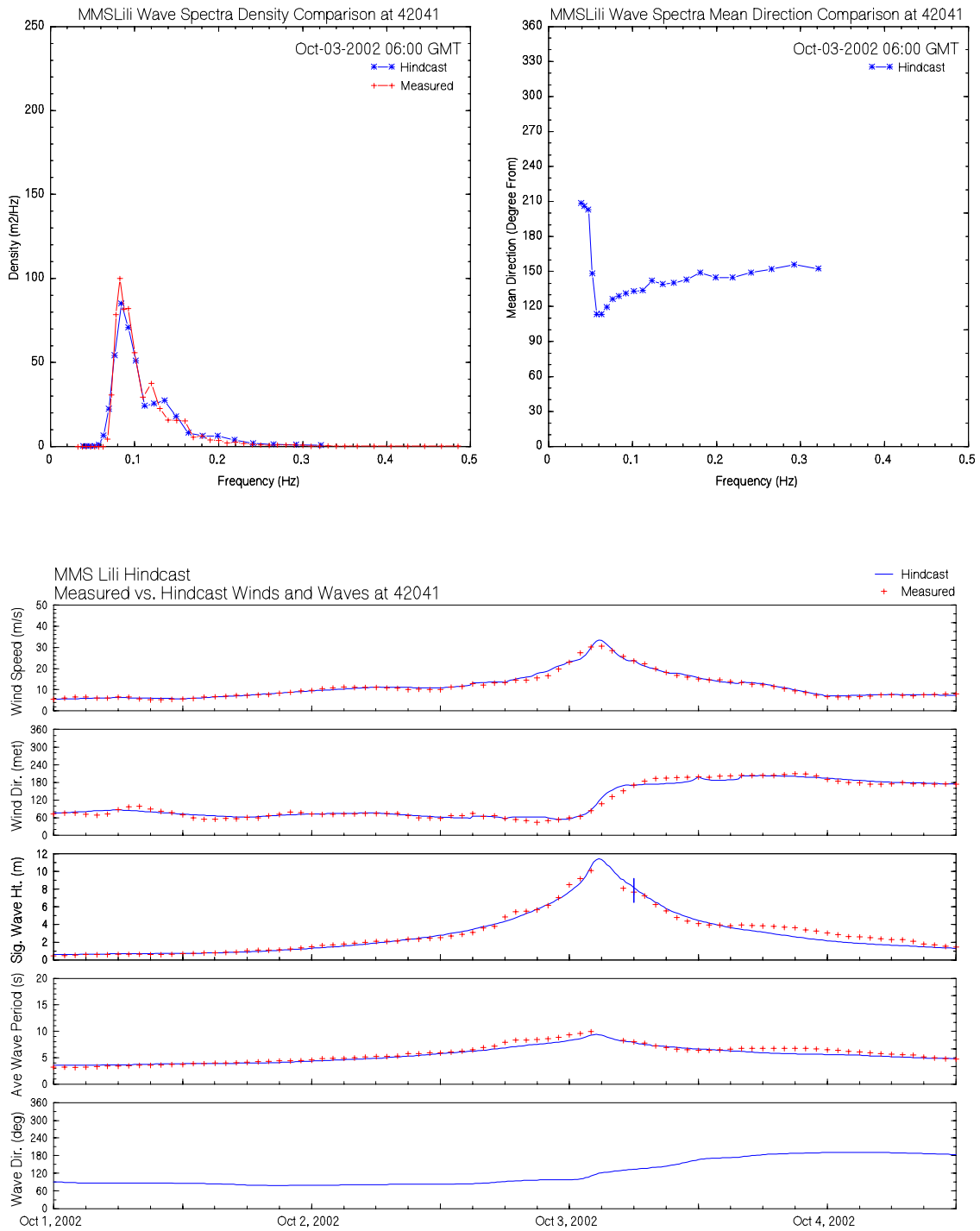


Figure 17 Wave spectra comparison at Buoy 42041 on Oct-03 06:00 GMT (3 hours after peak)

5.2 Altimeter Measurements

Altimeter measurements from the TOPEX and ERS-2 instruments were both providing data during the passage of Lili in the Gulf. Unfortunately, only the ERS-2 orbit allowed sampling of the core of Lili while in the Gulf. Figures 18 and 19 shows two altimeter trans-sections along with the nearest hindcast field (+/- 15 minutes). This is real-time ERS-2 (so called fast delivery product) and has not undergone the final quality control and processing as done for science-level data. The Oct-03-2002 04:00 GMT trans-section (Figure 14) shows excellent agreement in the core of Lili. The peak wave of 9.57 just outside the hindcast 10-meter contour is felt to be the best estimate of the peak conditions measured by the pass. Wave heights in the left-rear quadrant of Lili tend to be over-predicted; this is a characteristic of most 3rd generation wave models that put too much wave energy in this quadrant in tropical systems. The Oct-03-2002 17:00 GMT trans-section (Figure 15), after the landfall of Lili, shows excellent agreement between the measurements and the hindcast.

Hindcast of Hurricane Lili (2002)

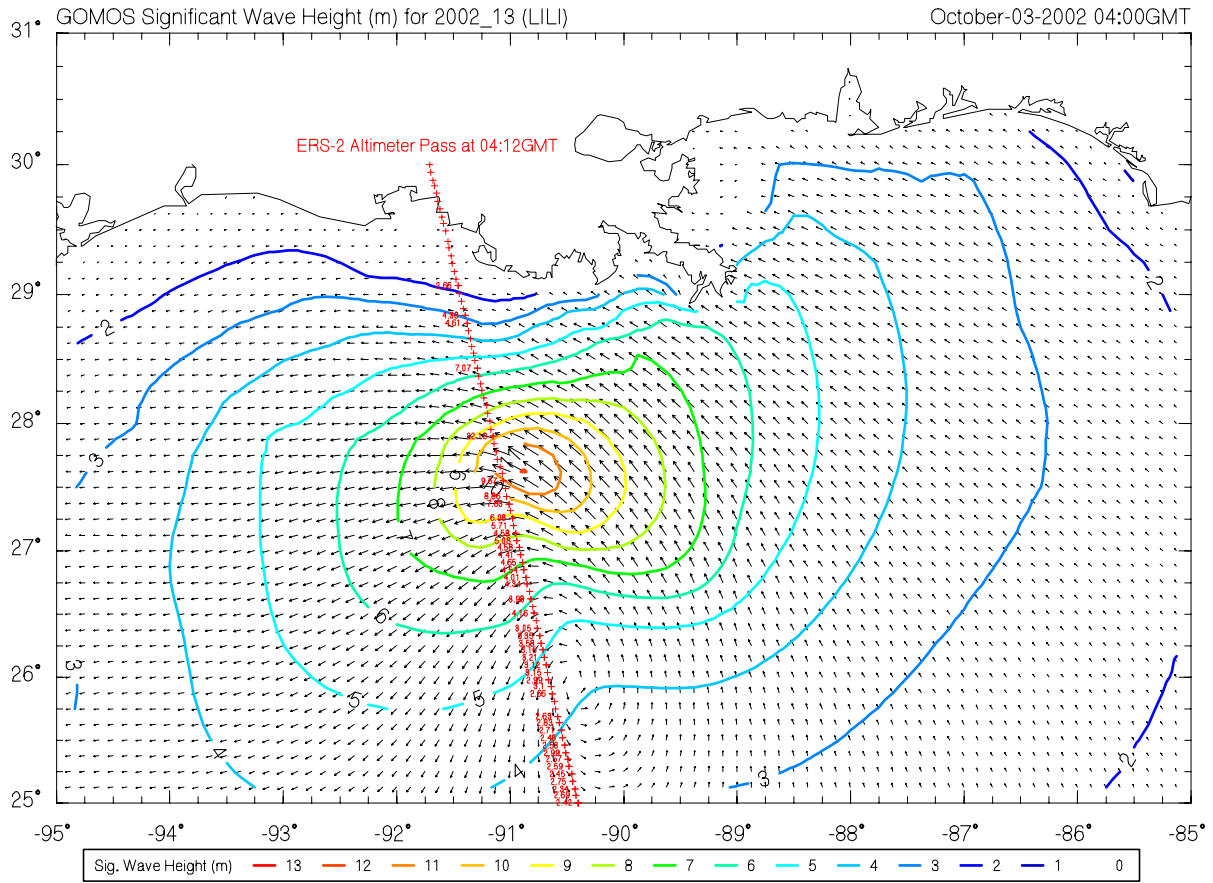


Figure 18 Comparison of hindcast significant wave height (m) and ERS-2 altimeter wave estimates at Oct-03-2002 04:00 GMT

Hindcast of Hurricane Lili (2002)

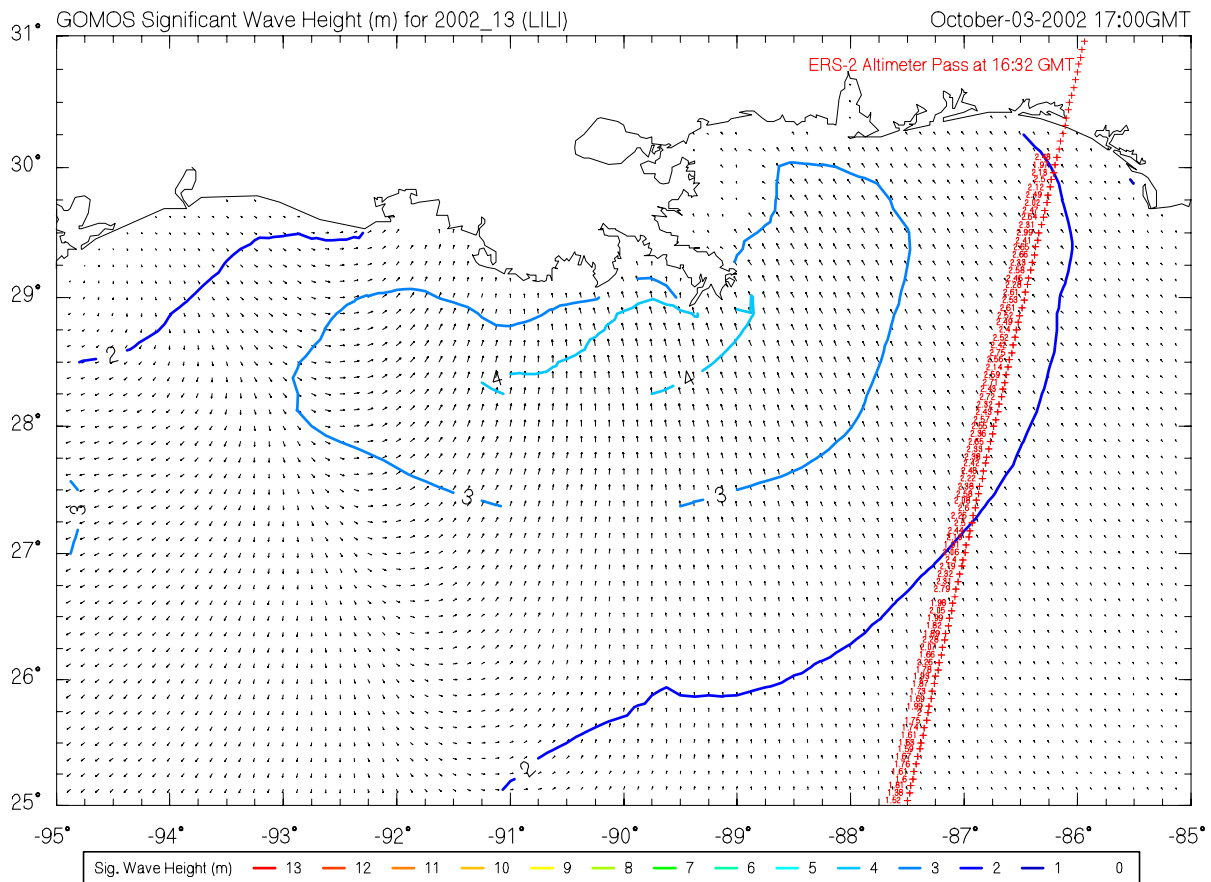


Figure 19 Comparison of hindcast significant wave height (m) and ERS-2 altimeter wave estimates at Oct-03-2002 17:00 GMT

6. DELIVERABLES

Along with this report, digital data from this hindcast is made available on a companion DVD. The DVD contains wind, wave, salinity, sea surface temperature and current results for all active grid points north of 26N and between 86W to 95W in the Gulf of Mexico. Files are in ASCII format with documentation provided on the DVD. Additional quality control and validation plots are also contained on the volume.

References

- Bunpapong, M., R. Reid, and R. Whitaker. 1985. An investigation of hurricane-induced forerunner surge in the Gulf of Mexico. Prepared for U.S. Army Engineer Waterways Experiment Station and the Coastal Engineering Research Center, Contract DACW39-82-K-0001, by Dept. of Oceanography, Texas A&M University, Ref. 85-2-T. Research conducted through Texas A&M Research Foundation, Project 4667, College Station, TX.
- Cardone, V. J., W. J. Pierson and E. G. Ward. 1976. Hindcasting the directional spectra of hurricane generated waves. J. of Petrol. Technol., 28, 385-394.
- Cardone, V. J. and D. B. Ross, 1979. State-of-the-art wave prediction methods and data requirements. Ocean Wave Climate ed. M. D. Earle and A. Malahoff. Plenum Publishing Corp., 1979, 61-91.
- Cardone, V. J., D. Szabo and F. J. Dello Stritto. Development of extreme wind and wave criteria for Hibernia. Second International Workshop on Wave Hindcasting and Forecasting, April 25-28, 1989, Vancouver, Canada.
- Cardone, V. J. and K. C. Ewans. Validation of the hindcast approach to the specification of wave conditions at the Maui location off the west coast of New Zealand. Preprints of the 3RD International Conference on Wave Hindcasting and Forecasting, Montreal, Quebec, May 9-22, 1992; 232-247. Published by Environment Canada, Downsview, Ontario.
- Cardone, V. J., C.V. Greenwood and J. A. Greenwood. 1992. Unified program for the specification of tropical cyclone boundary layer winds over surfaces of specified roughness. Contract Rep. CERC 92-1, U.S. Army Engrs. Wtrwy. Experiment Station, Vicksburg, Miss.
- Cardone, V. J. and C. K. Grant. 1994. Southeast Asia meteorological and oceanographic hindcast study (SEAMOS). OSEA 94132. 10th Offshore Southeast Asia Conference, 6-9 December, 1994.
- Cardone, V. J., R. E. Jensen, D. T. Resio, V. R. Swail and A. T. Cox. 1996. Evaluation of contemporary ocean wave models in rare extreme events: Halloween storm of October, 1991; Storm of the century of March, 1993. J. of Atmos. and Ocean. Tech., 13, 198-230.
- Cardone, V. J. and D. T. Resio, 1998. An assessment of wave modeling technology. Preprints of 5th International Workshop on Wave Hindcasting and Forecasting. Melbourne, Fl. January 26-30, 1998.
- Cardone, V. J. and D. T. Resio. 1998. An assessment of wave modeling technology. 5th International Workshop on Wave Hindcasting and Forecasting, Jan. 26-30, Melbourne,

- Chow, S. H., 1971. A study of the wind field in the planetary boundary layer of a moving tropical cyclone. Master of Science Thesis in Meteorology, School of Engineering and Science, New York University, New York, N.Y.
- Cox, A.T. and V.R. Swail. A Global Wave Hindcast over the Period 1958-1997: Validation and Climate Assessment. *JGR (Oceans)*, Vol. 106, No. C2, pp. 2313-2329, February 2001.
- Eid, B., V. J. Cardone, and V. Swail. Beaufort Sea extreme wind/wave hindcast study. Preprints of the 3RD International Conference on Wave Hindcasting and Forecasting, Montreal, Quebec, May 9-22, 1992; 351-361. Published by Environment Canada, Downsview, Ontario.
- Forristall, G.Z., R. C. Hamilton and V. J. Cardone, 1977. Continental shelf currents in tropical storm Delia: observations and theory. *J. of Phys. Oceanog.* 7, 532-546.
- Forristall, G. Z., E. G. Ward, V. J. Cardone, and L. E. Borgman. 1978. The directional spectra and kinematics of surface waves in Tropical Storm Delia. *J. of Phys. Oceanog.*, 8, 888-909.
- Forristall, G. Z., 1980. A two-layer model for hurricane driven currents on an irregular grid. *J. Phys. Oceanog.*, 10, 9, 1417-1438.
- Holland, G. J., 1980. An analytical model of the wind and pressure profiles in hurricanes. *Mon. Wea. Rev.* 1980, 108, 1212-1218.
- Khandekar, M. L., R. Lalbeharry and V. J. Cardone. 1994. The performance of the Canadian spectral ocean wave model (CSOWM) during the Grand Banks ERS-1 SAR wave spectra validation experiment. *Atmosphere-Oceans*, 32, 31-60.
- Ross, D. B. and V. J. Cardone, 1978. A comparison of parametric and spectral hurricane wave prediction products. *Turbulent Fluxes through the Sea Surface, Wave Dynamics, and Prediction*, A. Favre and K. Hasselmann, editors, 647-665.
- Shapiro, L. J., 1983. The asymmetric boundary layer flow under a translating hurricane. *J. of Atm. Sci.* 39 (February).
- Swail, V. K., V. J. Cardone and B. Eid. Extreme wave climate off the west coast of Canada. Preprint Volume of the AMS Conference on Meteorology and Oceanography of the Coastal Zone. May 6-10, 1991, Key Biscayne, Florida.
- Swail, V.R. and A.T. Cox. On the use of NCEP/NCAR Reanalysis Surface Marine Wind Fields for a Long Term North Atlantic Wave Hindcast *J. Atmo. Tech.* Vol. 17, No. 4, pp. 532-545, 2000.
- Thompson, E. F. and V. J. Cardone. 1996. Practical modeling of hurricane surface wind fields. *ASCE J. of Waterway, Port, Coastal and Ocean Engineering.* 122, 4, 195-205.

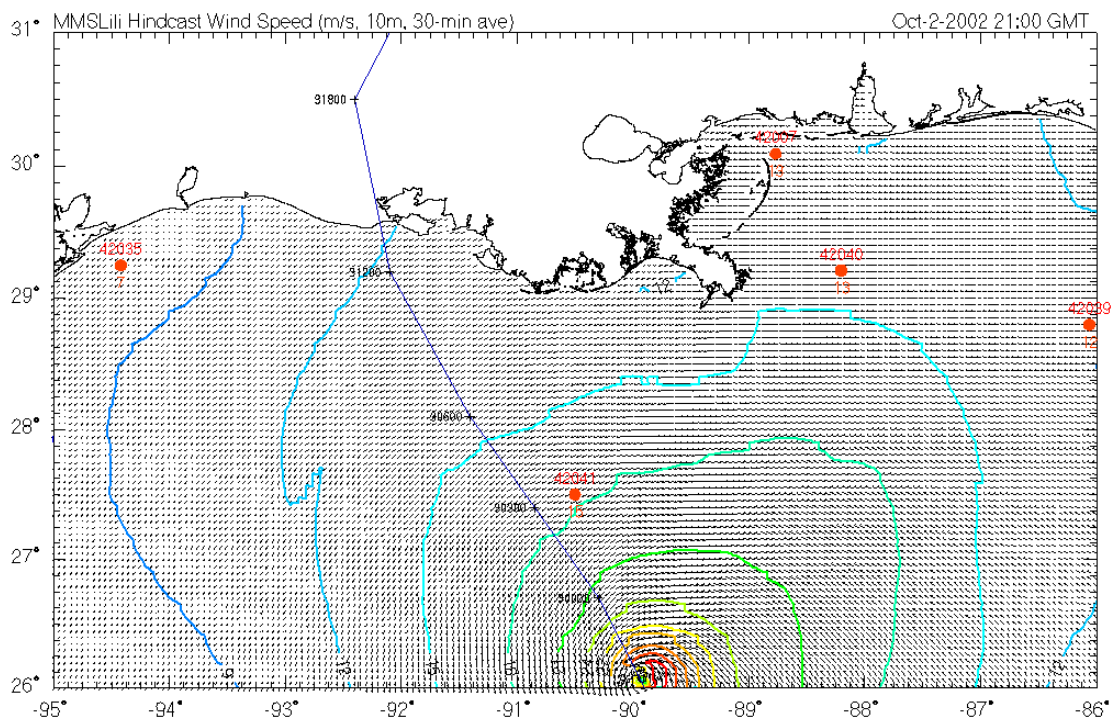
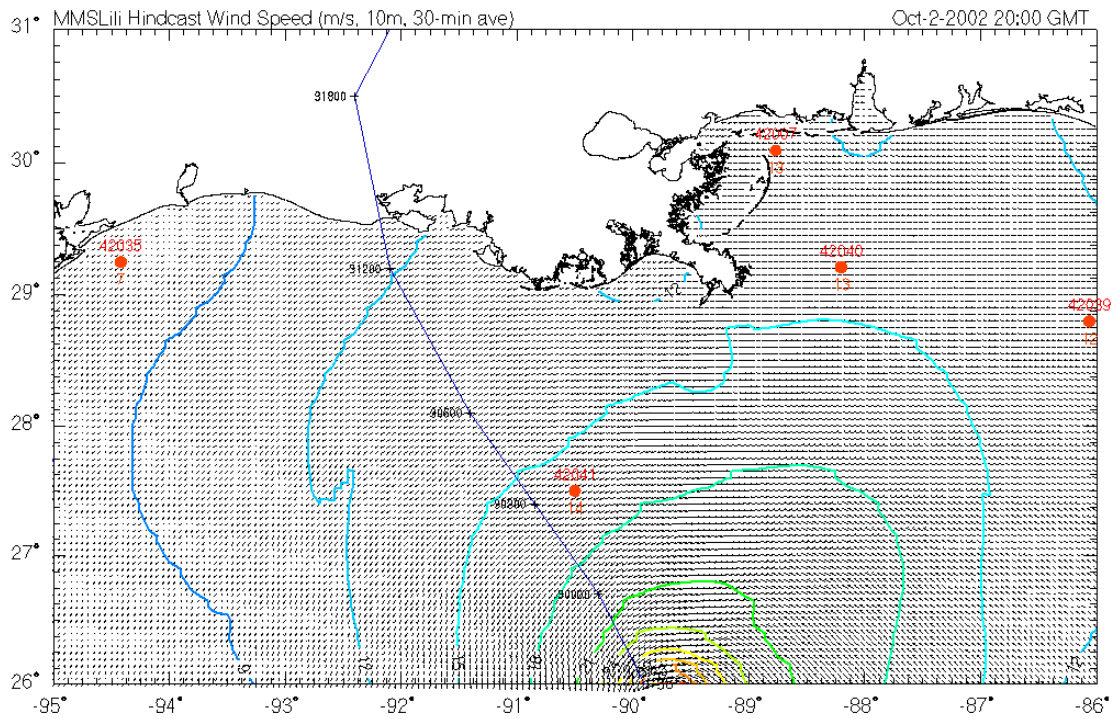
APPENDIX A. Hindcast Track and Intensity of Hurricane Lili

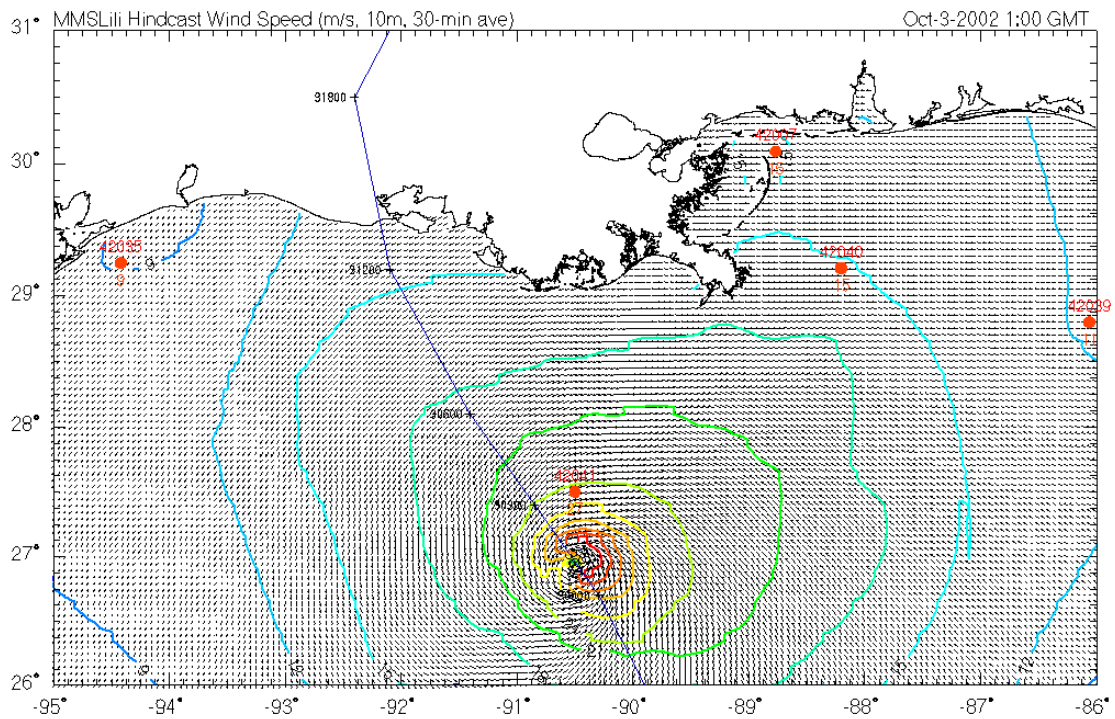
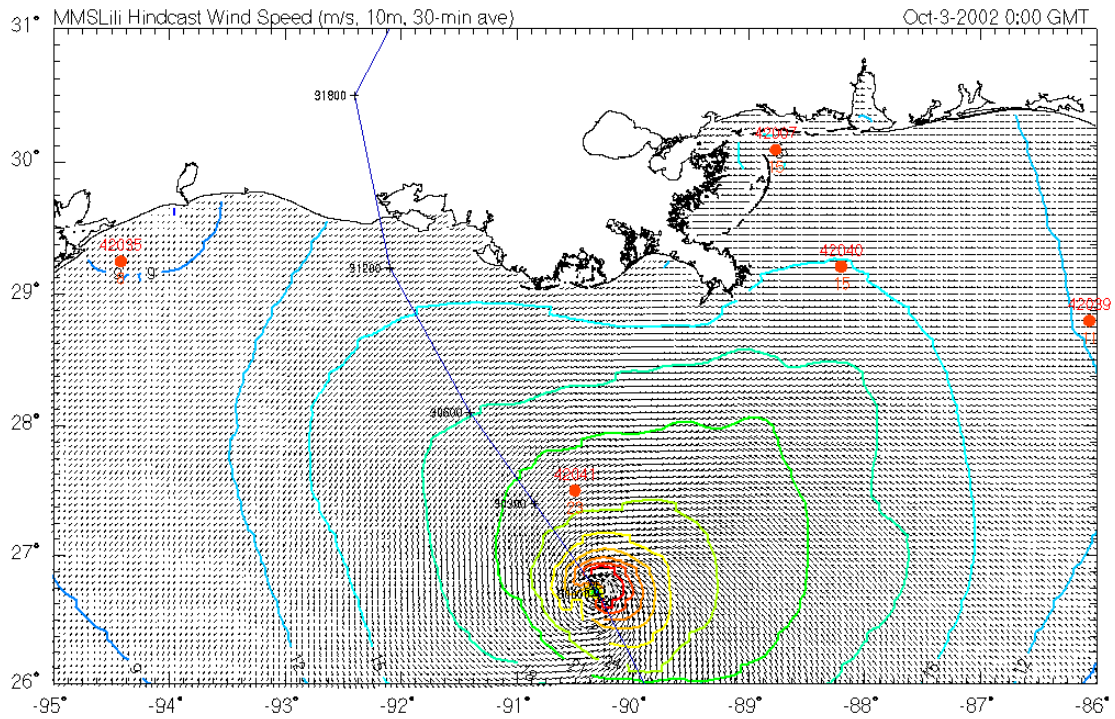
From National Hurricane Center Tropical Cyclone Report

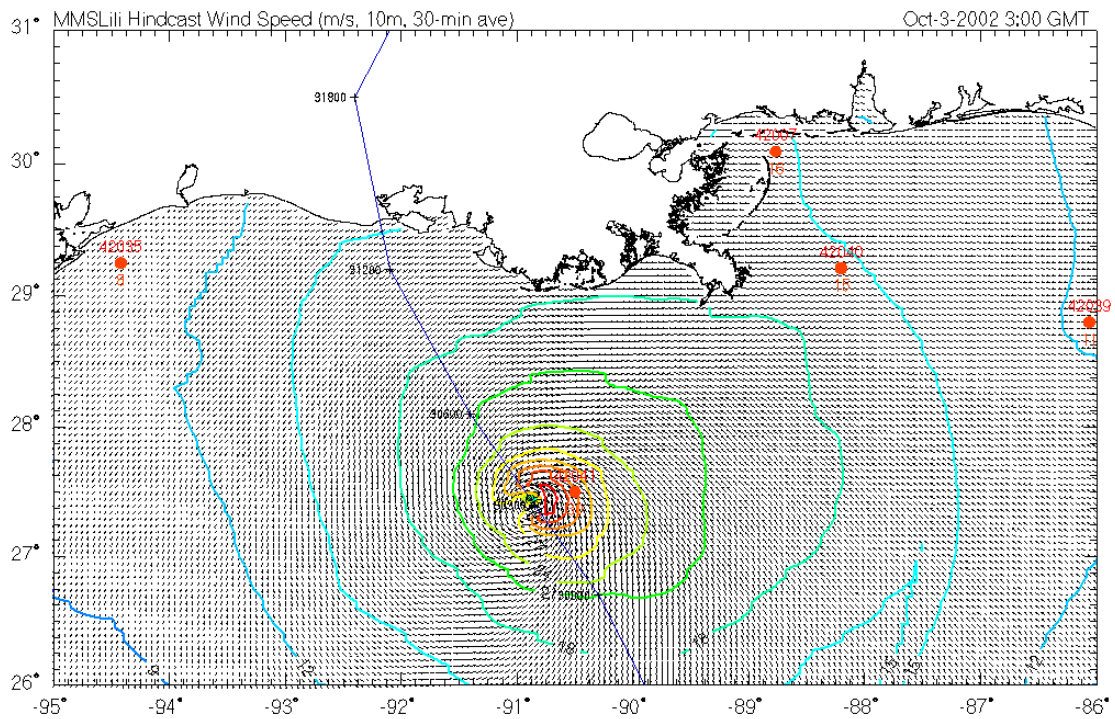
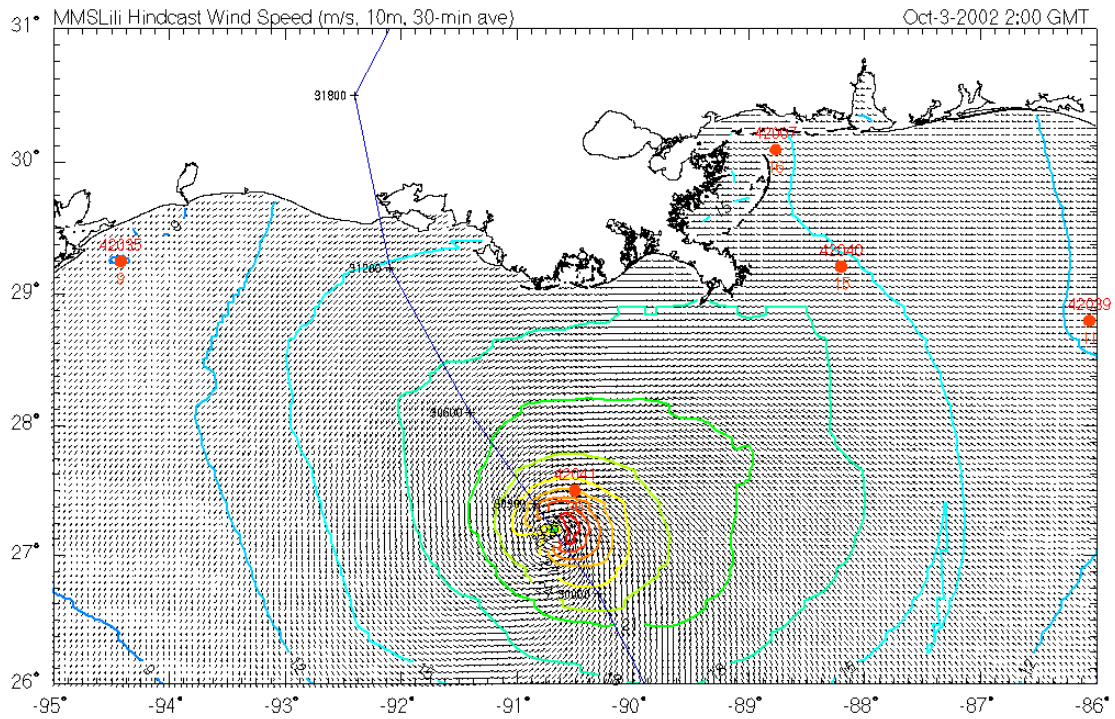
| Date/Time (UTC) | Position | | Pressure (mb) | Wind Speed (kt) | Stage |
|--------------------|--------------|--------------|------------------|--------------------|---------------------|
| | Lat. (°N) | Lon. (°W) | | | |
| 21 / 1800 | 10.2 | 44.6 | 1009 | 25 | tropical depression |
| 22 / 0000 | 10.3 | 46.5 | 1007 | 30 | " |
| 22 / 0600 | 10.8 | 48.5 | 1006 | 30 | " |
| 22 / 1200 | 11.2 | 50.4 | 1006 | 30 | " |
| 22 / 1800 | 11.8 | 52.2 | 1005 | 30 | " |
| 23 / 0000 | 12.1 | 54.6 | 1005 | 35 | tropical storm |
| 23 / 0600 | 12.2 | 56.8 | 1005 | 40 | " |
| 23 / 1200 | 12.4 | 58.7 | 1004 | 45 | " |
| 23 / 1800 | 12.5 | 60.4 | 1005 | 50 | " |
| 24 / 0000 | 12.7 | 62.1 | 1006 | 50 | " |
| 24 / 0600 | 12.8 | 63.7 | 1006 | 50 | " |
| 24 / 1200 | 13.0 | 64.9 | 1004 | 60 | " |
| 24 / 1800 | 13.2 | 66.0 | 1007 | 50 | " |
| 25 / 0000 | 13.5 | 66.9 | 1008 | 35 | " |
| 25 / 0600 | 13.7 | 67.5 | 1008 | 35 | " |
| 25 / 1200 | 14.0 | 68.2 | 1008 | 40 | tropical wave |
| 25 / 1800 | 14.2 | 68.9 | 1007 | 40 | " |
| 26 / 0000 | 14.5 | 69.8 | 1007 | 35 | " |
| 26 / 0600 | 14.9 | 71.0 | 1007 | 35 | " |
| 26 / 1200 | 15.3 | 72.2 | 1007 | 30 | " |
| 26 / 1800 | 15.6 | 73.0 | 1006 | 30 | " |
| 27 / 0000 | 15.7 | 73.5 | 1006 | 30 | tropical depression |
| 27 / 0600 | 15.9 | 74.0 | 1006 | 30 | " |
| 27 / 1200 | 16.1 | 74.6 | 1003 | 35 | tropical storm |
| 27 / 1800 | 16.7 | 75.0 | 1004 | 40 | " |
| 28 / 0000 | 17.4 | 75.1 | 999 | 45 | " |
| 28 / 0600 | 17.5 | 75.6 | 999 | 45 | " |
| 28 / 1200 | 18.1 | 75.4 | 1002 | 45 | " |
| 28 / 1800 | 18.5 | 75.7 | 1003 | 45 | " |
| 29 / 0000 | 18.8 | 76.1 | 1001 | 45 | tropical storm |
| 29 / 0600 | 18.8 | 76.8 | 999 | 40 | " |
| 29 / 1200 | 18.7 | 77.2 | 994 | 45 | " |
| 29 / 1800 | 18.7 | 77.6 | 994 | 50 | " |
| 30 / 0000 | 19.0 | 78.1 | 993 | 55 | " |

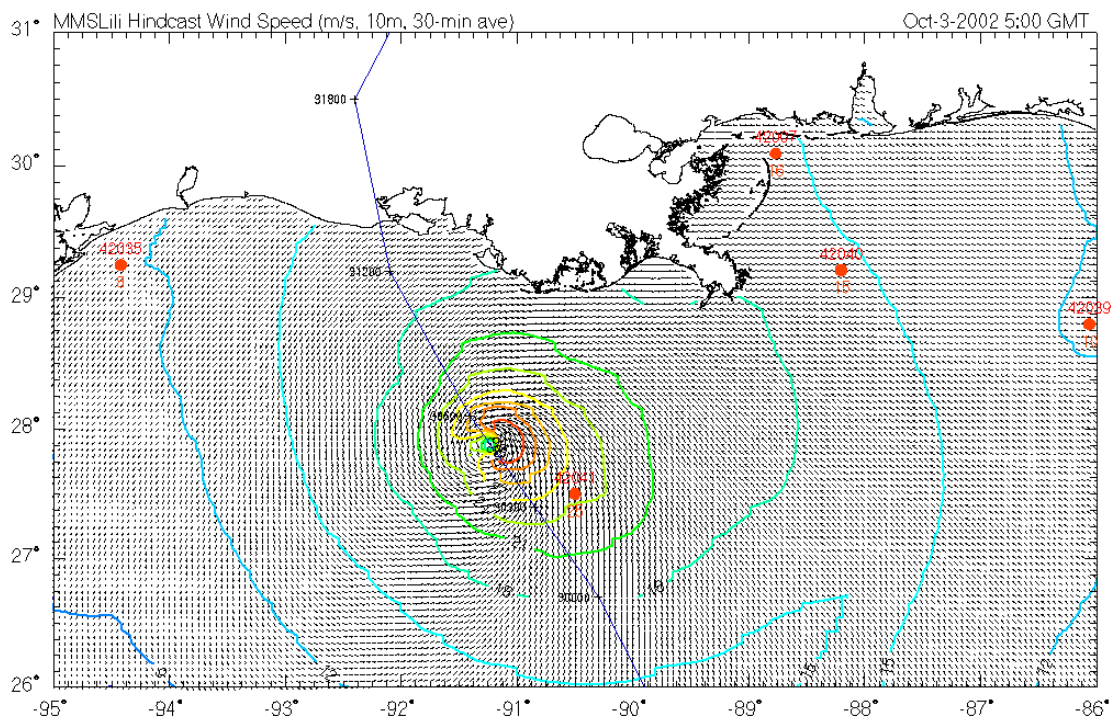
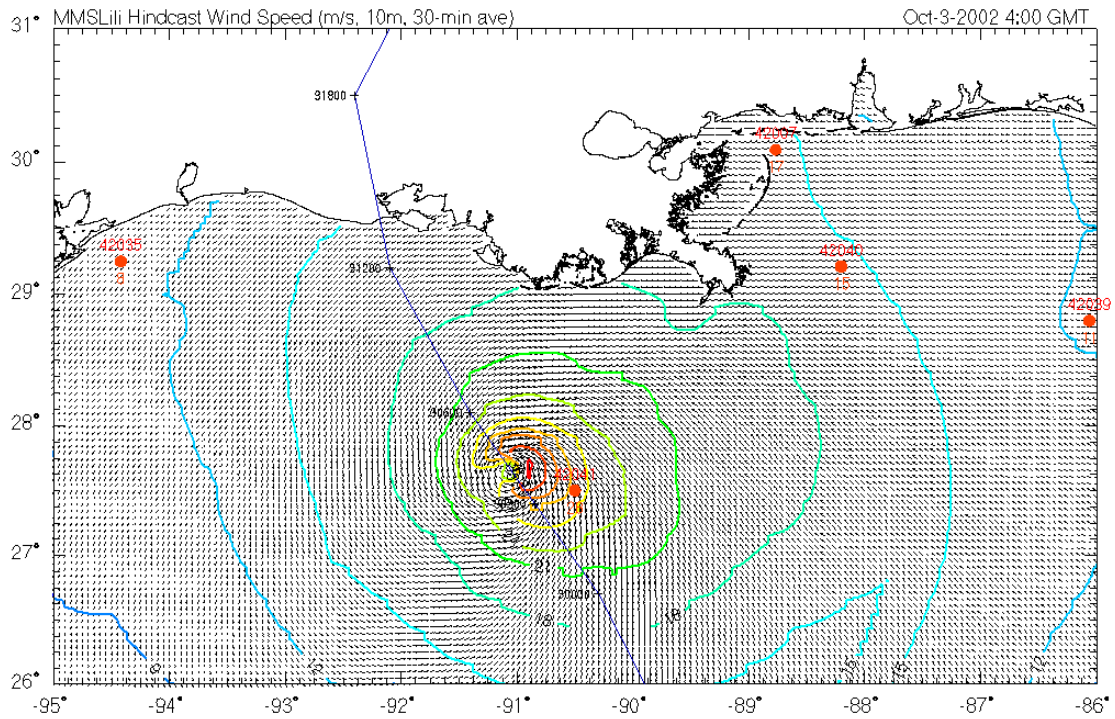
| | | | | | |
|-----------|------|------|-----|-----|--|
| 30 / 0600 | 19.1 | 78.7 | 990 | 60 | " |
| 30 / 1200 | 19.6 | 79.6 | 986 | 65 | hurricane |
| 30 / 1800 | 20.0 | 80.3 | 984 | 65 | " |
| 01 / 0000 | 20.5 | 81.1 | 978 | 70 | " |
| 01 / 0600 | 21.0 | 82.2 | 970 | 75 | " |
| 01 / 1200 | 21.6 | 83.2 | 971 | 90 | " |
| 01 / 1800 | 22.4 | 84.4 | 971 | 90 | " |
| 02 / 0000 | 23.0 | 85.7 | 967 | 90 | " |
| 02 / 0600 | 23.6 | 87.2 | 954 | 100 | " |
| 02 / 1200 | 24.4 | 88.3 | 954 | 110 | " |
| 02 / 1800 | 25.4 | 89.5 | 941 | 120 | " |
| 03 / 0000 | 26.7 | 90.3 | 940 | 125 | " |
| 03 / 0600 | 28.1 | 91.4 | 957 | 105 | " |
| 03 / 1200 | 29.2 | 92.1 | 962 | 80 | " |
| 03 / 1800 | 30.5 | 92.4 | 976 | 60 | tropical storm |
| 04 / 0000 | 31.9 | 92.1 | 985 | 40 | " |
| 04 / 0600 | 33.5 | 91.4 | 994 | 30 | tropical depression |
| 04 / 1200 | 35.8 | 90.0 | 997 | 25 | " |
| 04 / 1800 | | | | | absorbed by extratropical low |
| 02 / 2013 | 25.9 | 89.9 | 938 | 125 | minimum pressure |
| 30 / 1400 | 19.7 | 79.8 | 986 | 65 | landfall-Little Cayman and Cayman Brac |
| 01 / 1100 | 21.3 | 83.0 | 971 | 90 | landfall-Isle of Youth, Cuba |
| 01 / 1400 | 22.1 | 84.0 | 971 | 90 | landfall-Pinar del Rio Province, Cuba |
| 03 / 1300 | 29.5 | 92.2 | 963 | 80 | landfall-near Intracoastal City, LA |

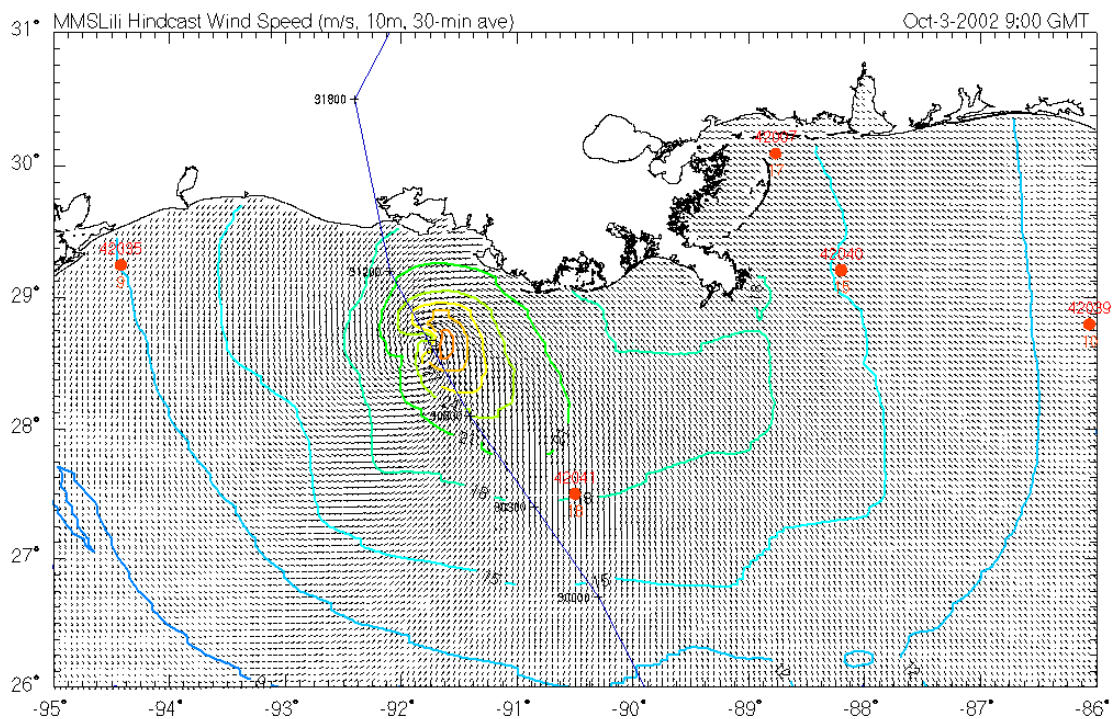
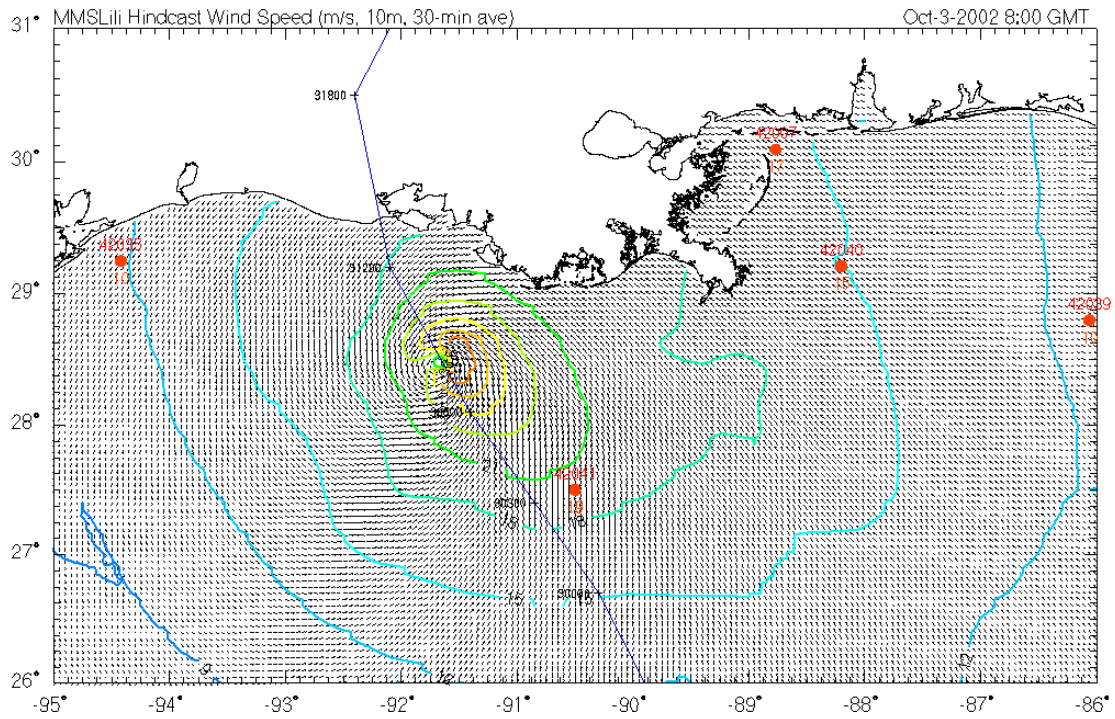
APPENDIX B. Vector Field Plots of Hindcast and Measured Winds

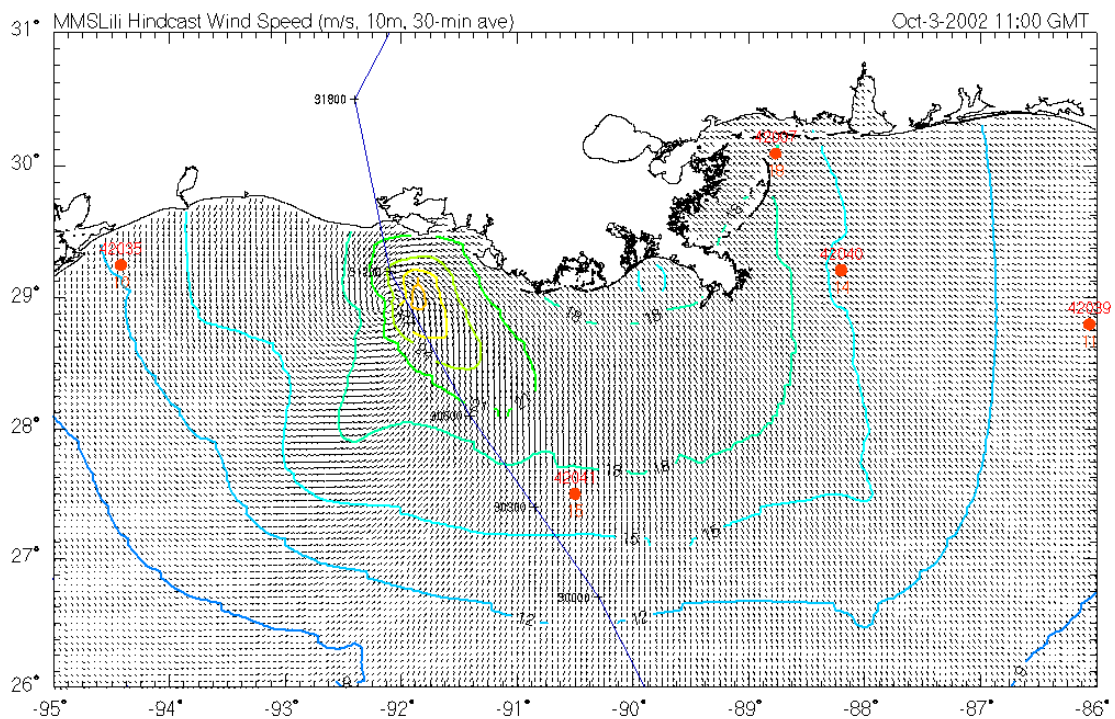
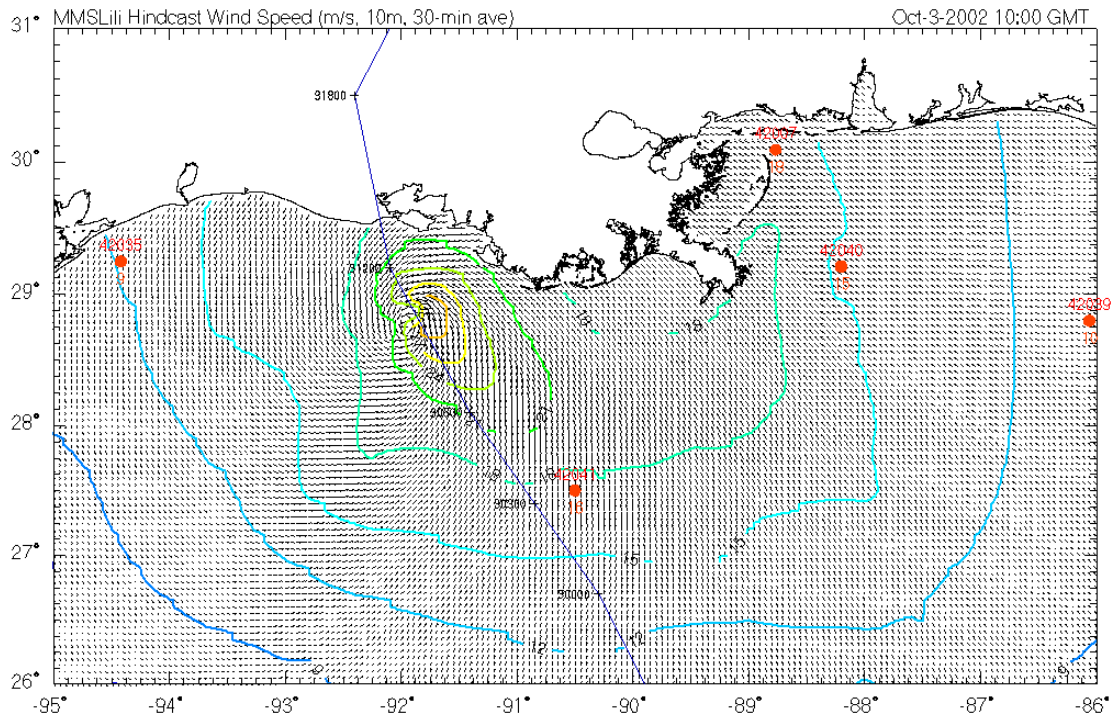


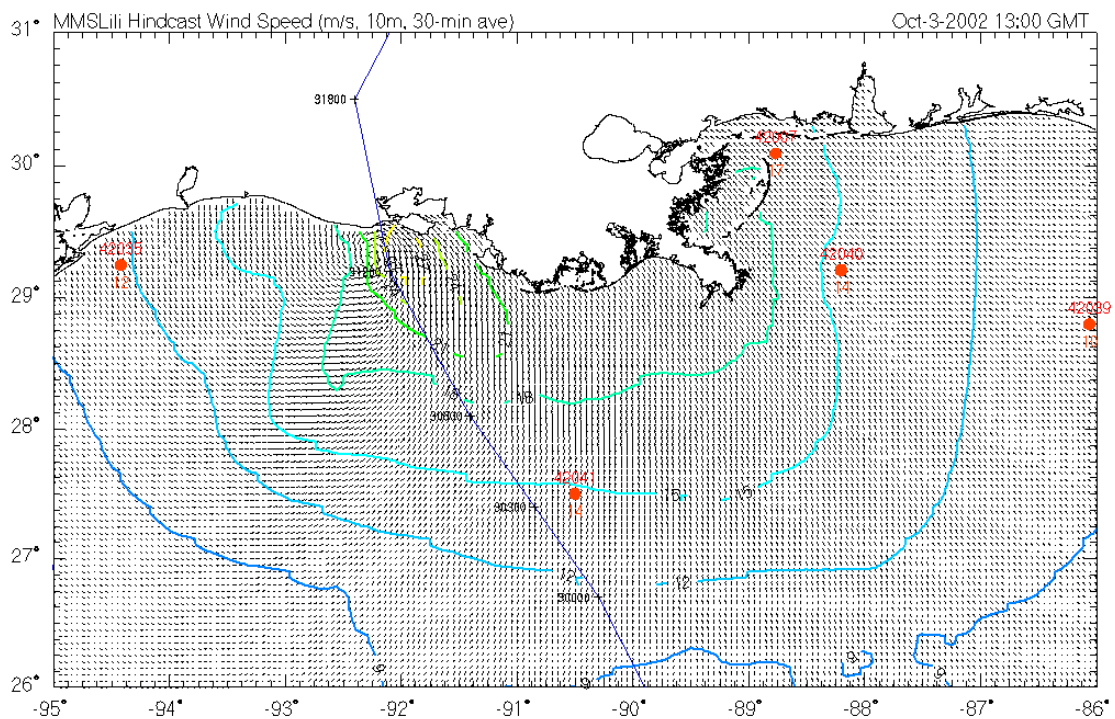
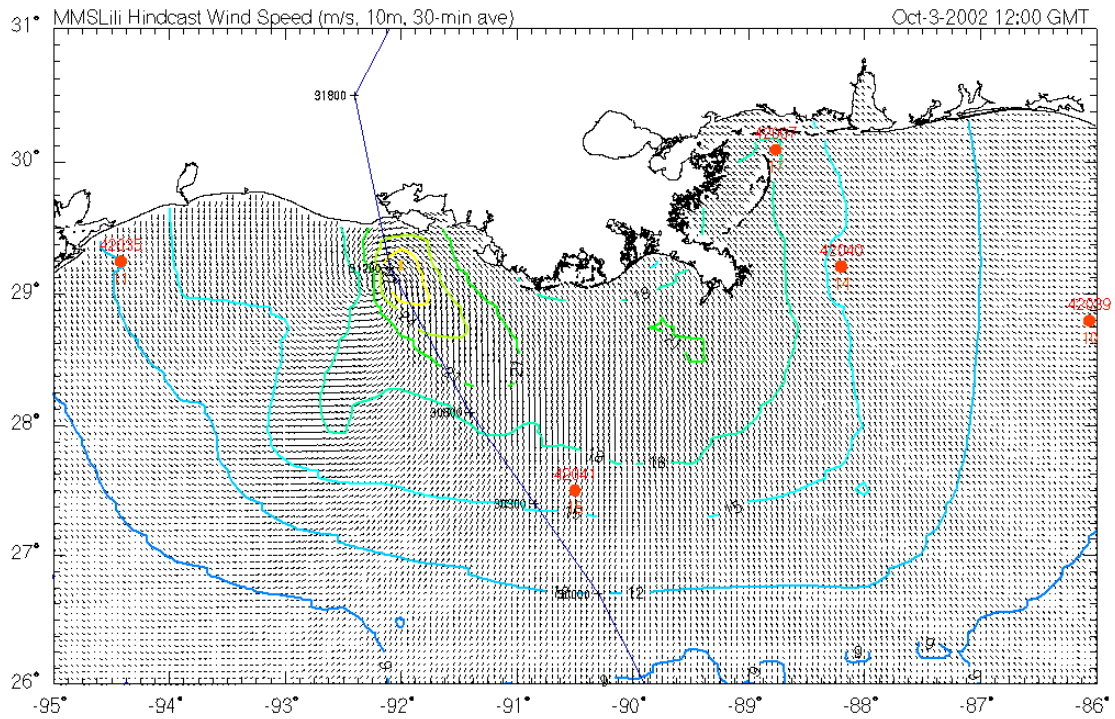


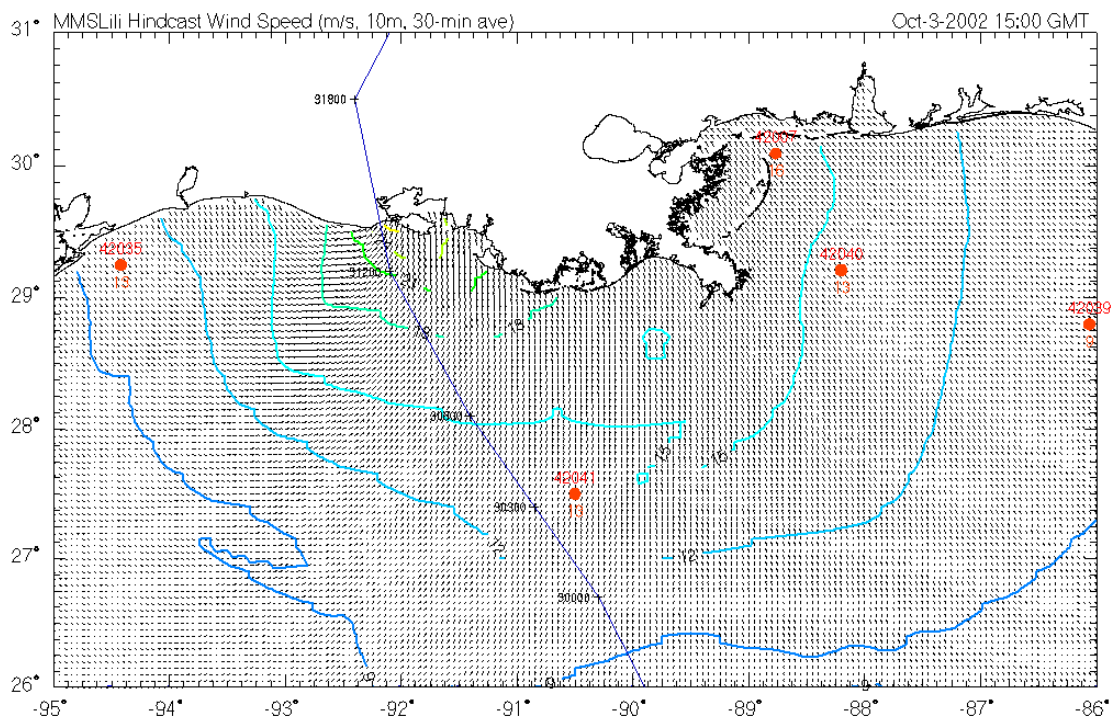
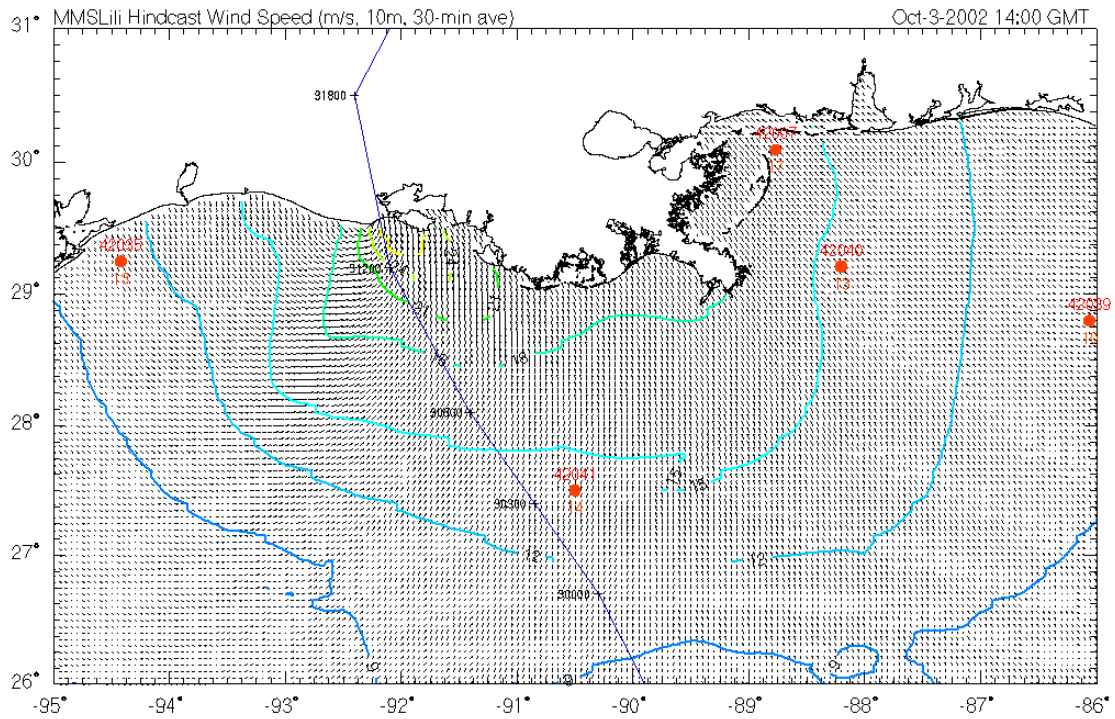


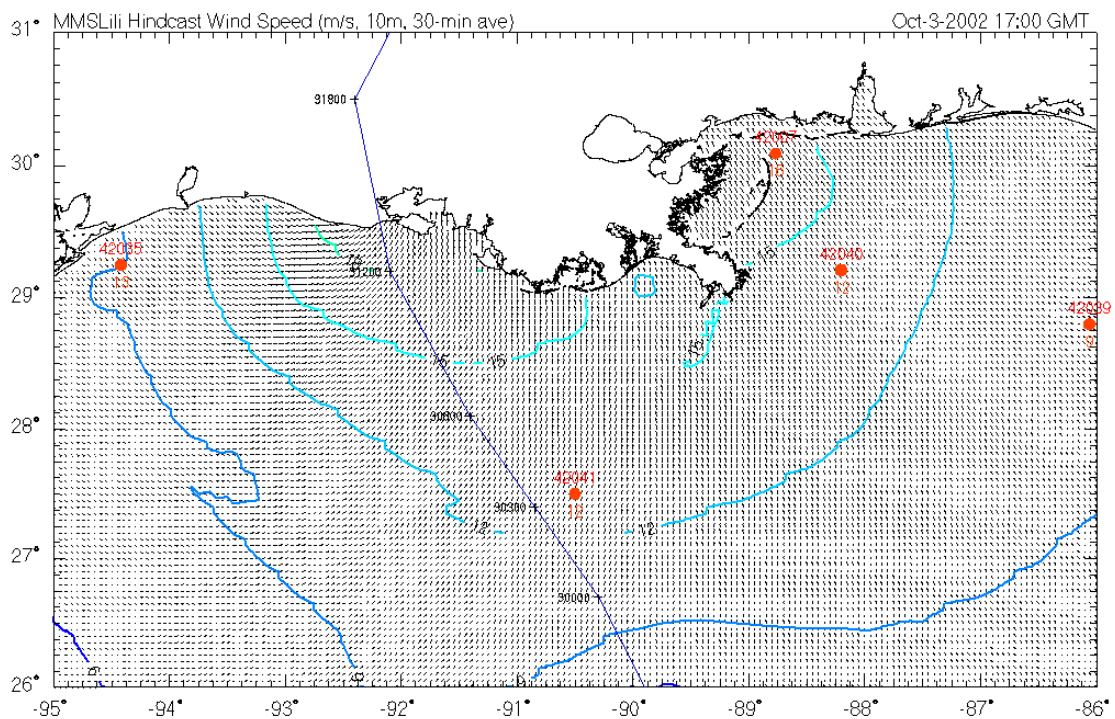
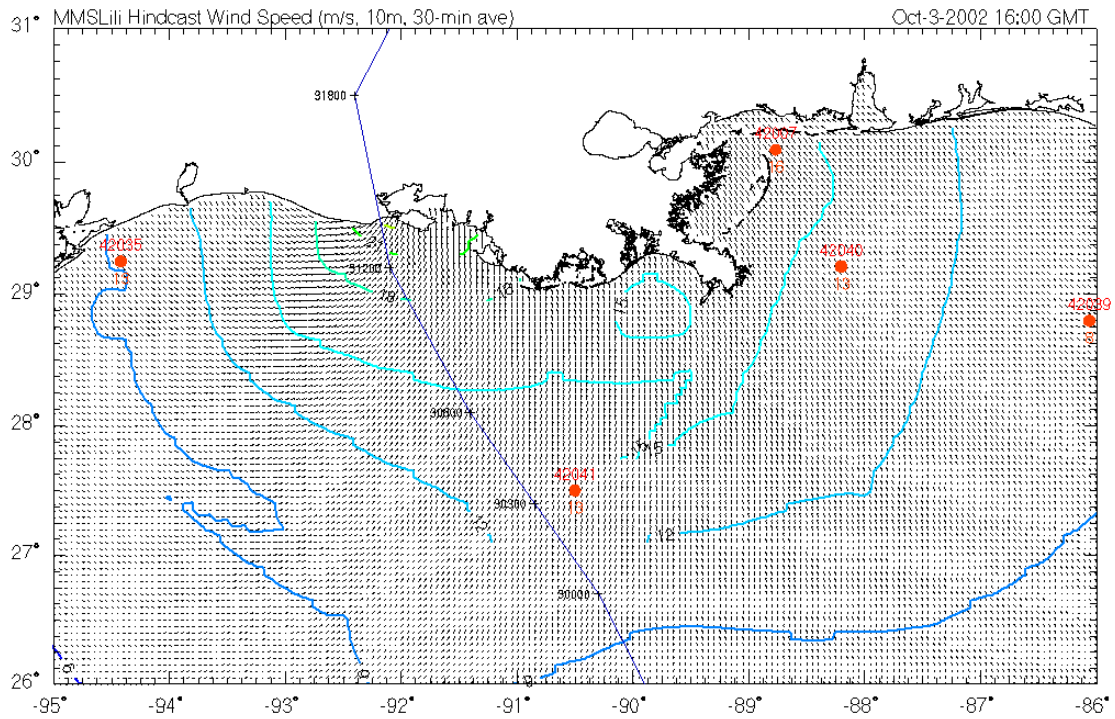


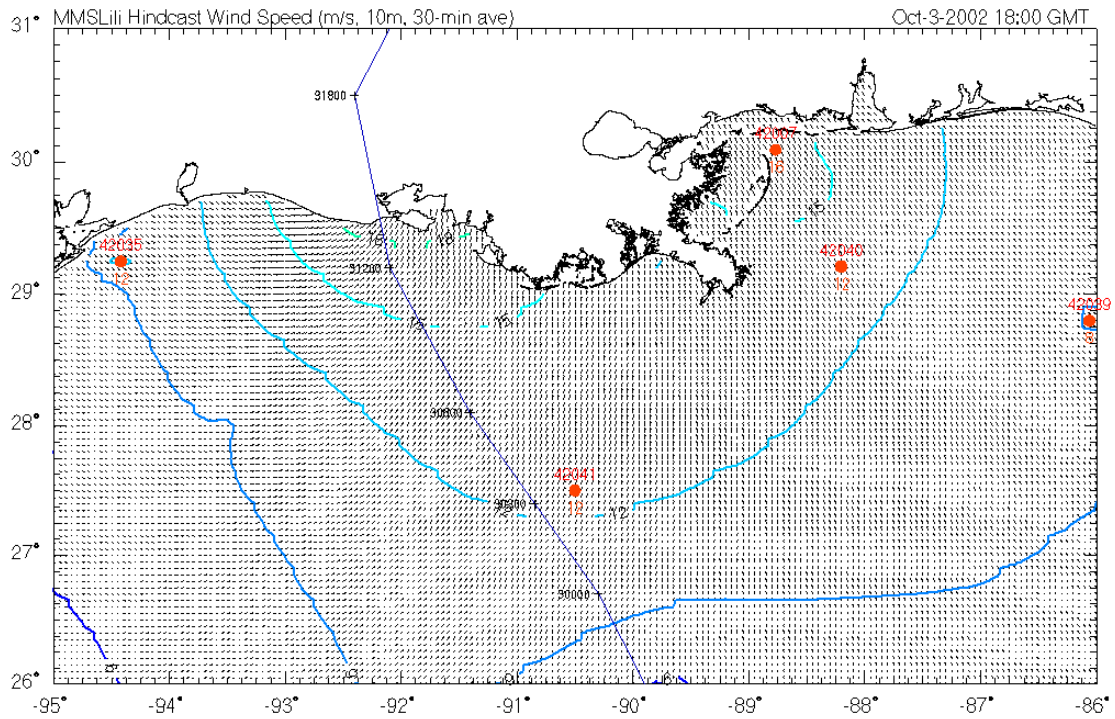




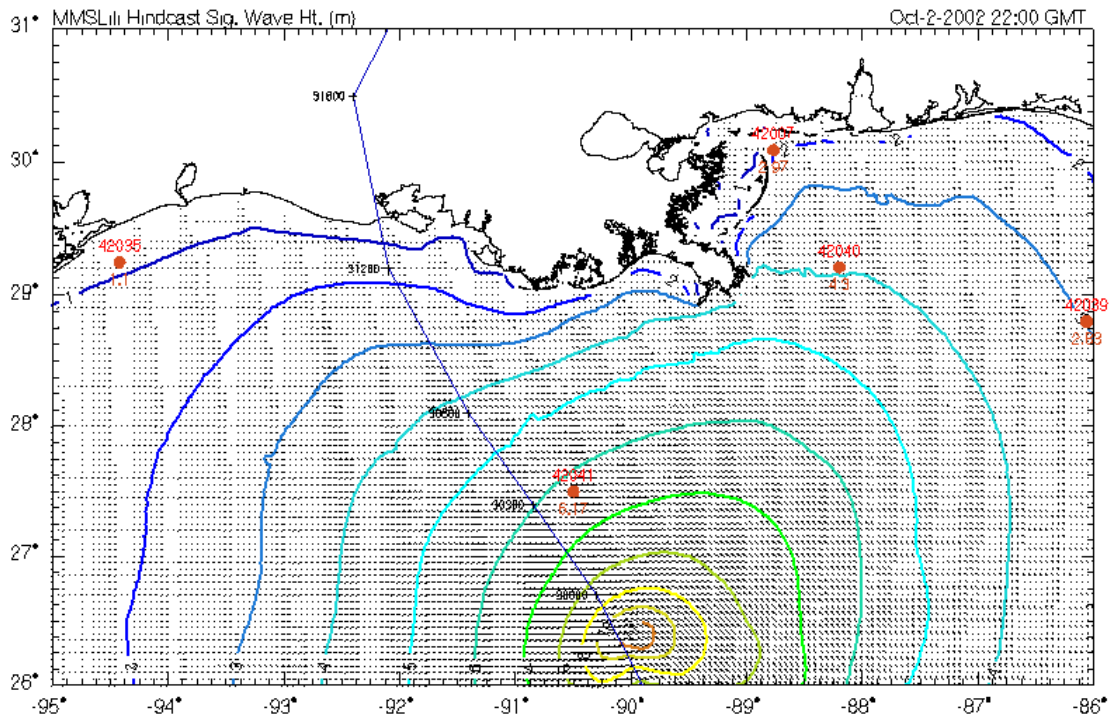


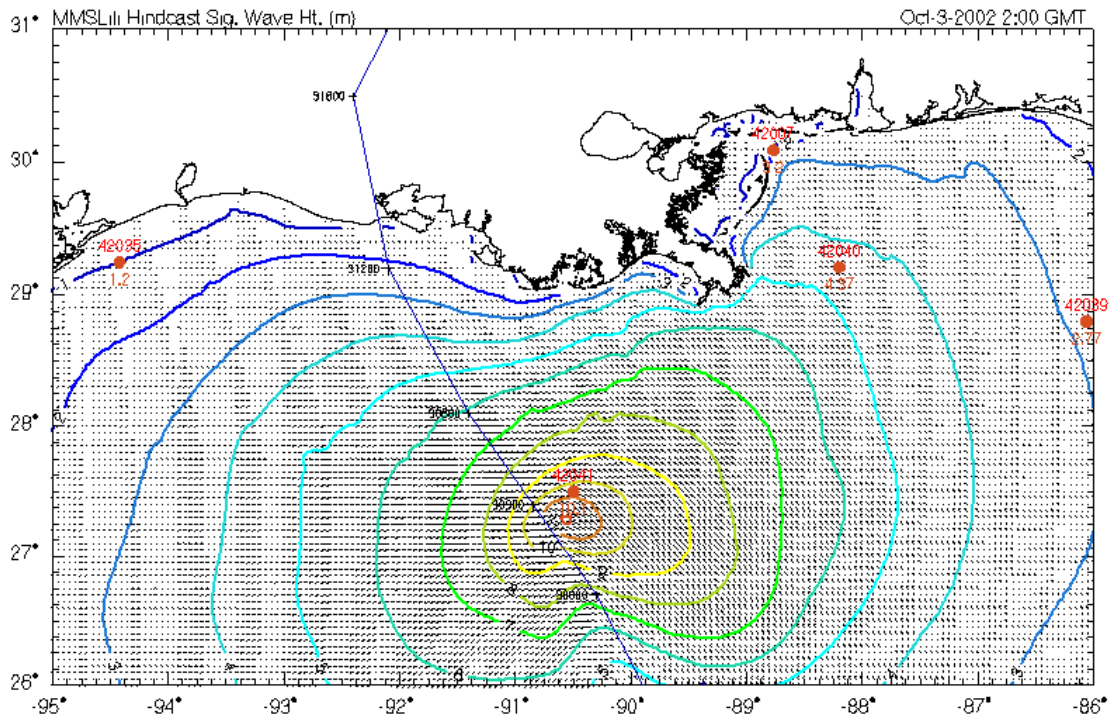


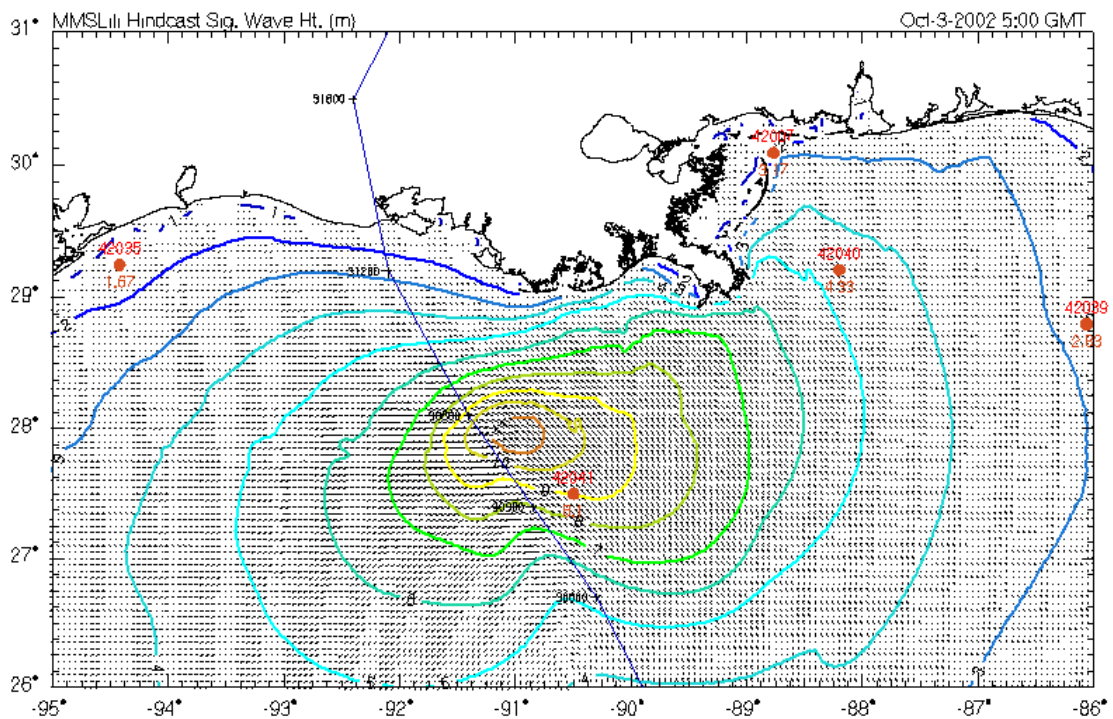
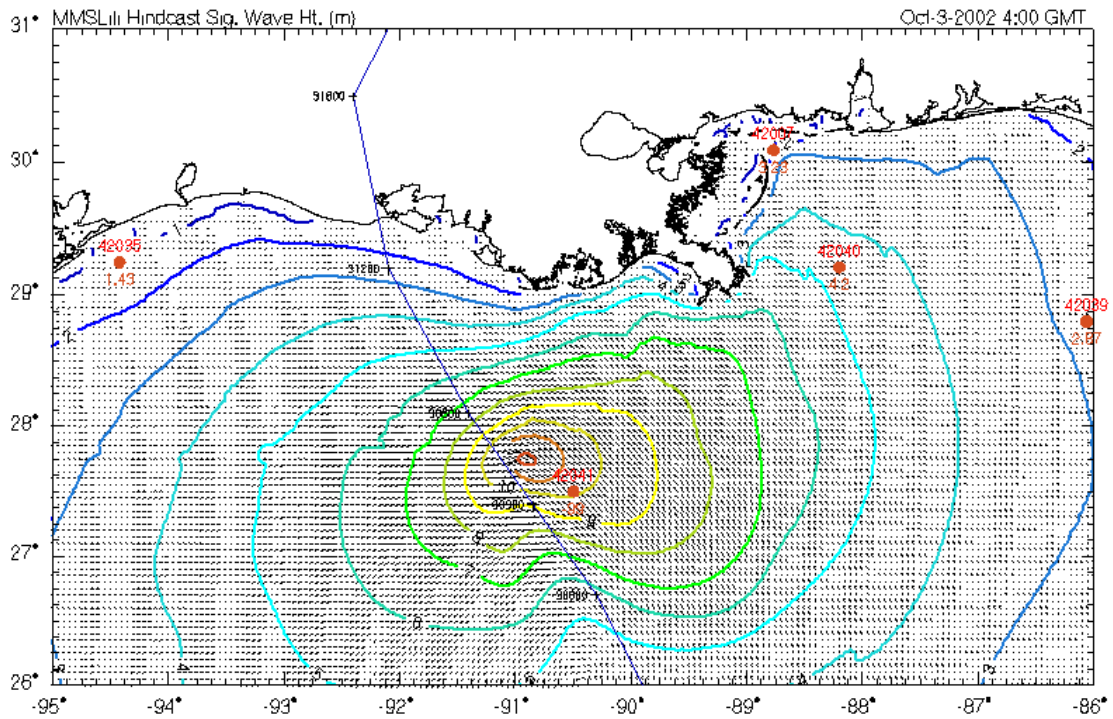


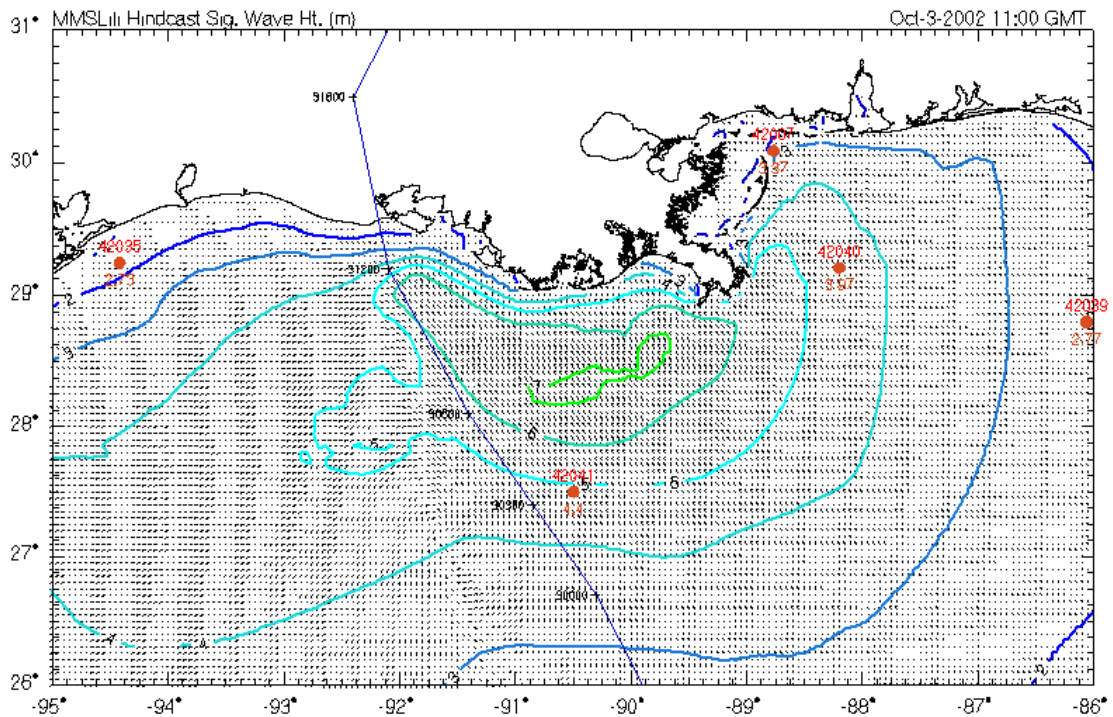
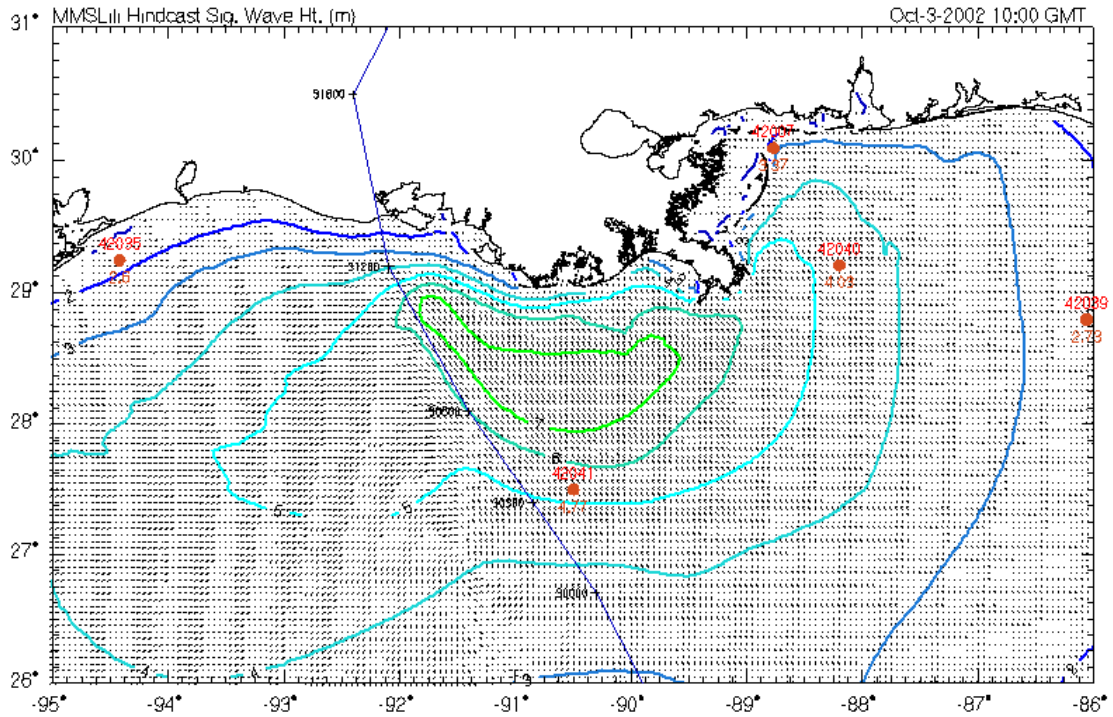


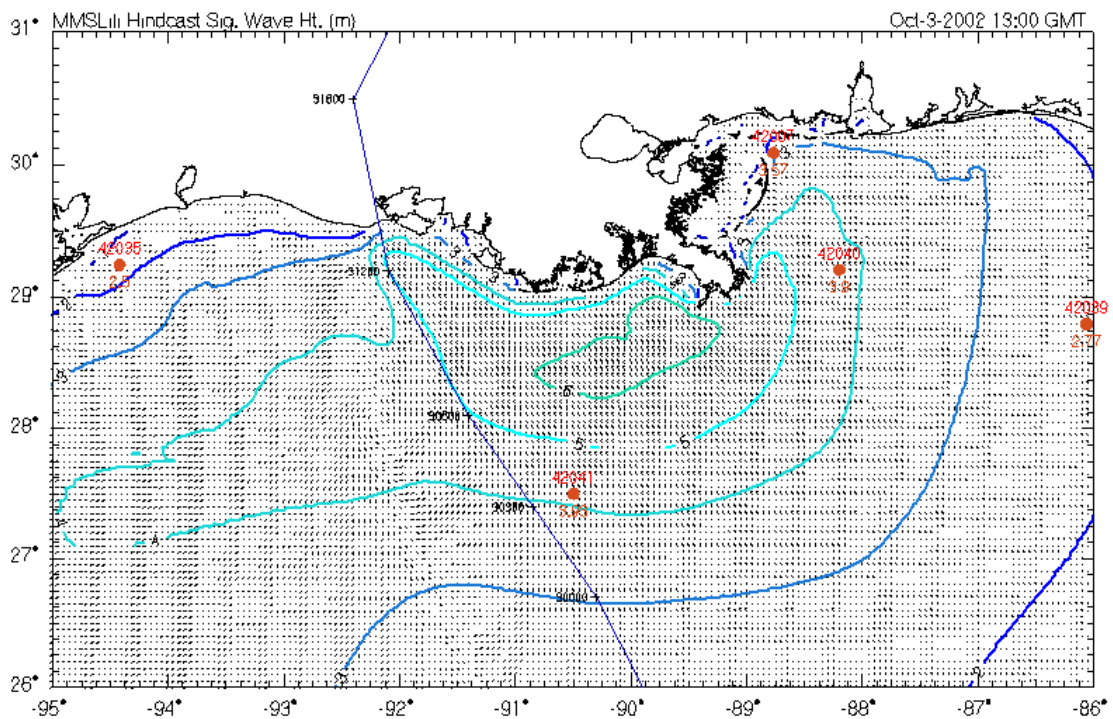
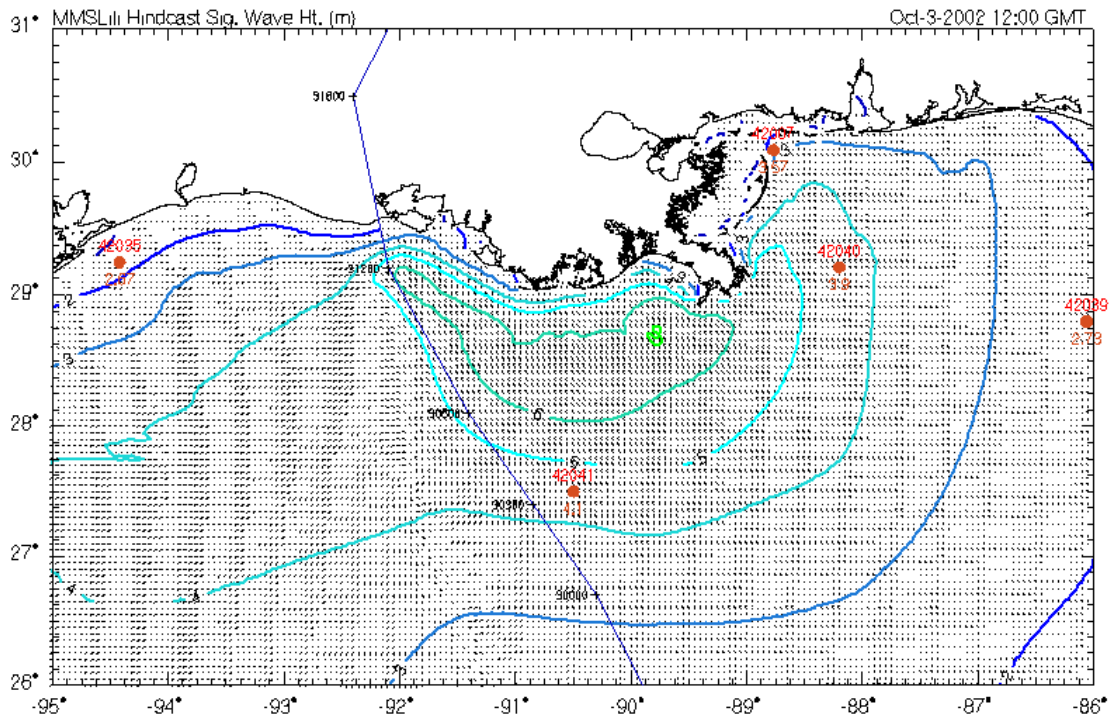
APPENDIX C. Vector Field Plots of Hindcast and Measured Waves

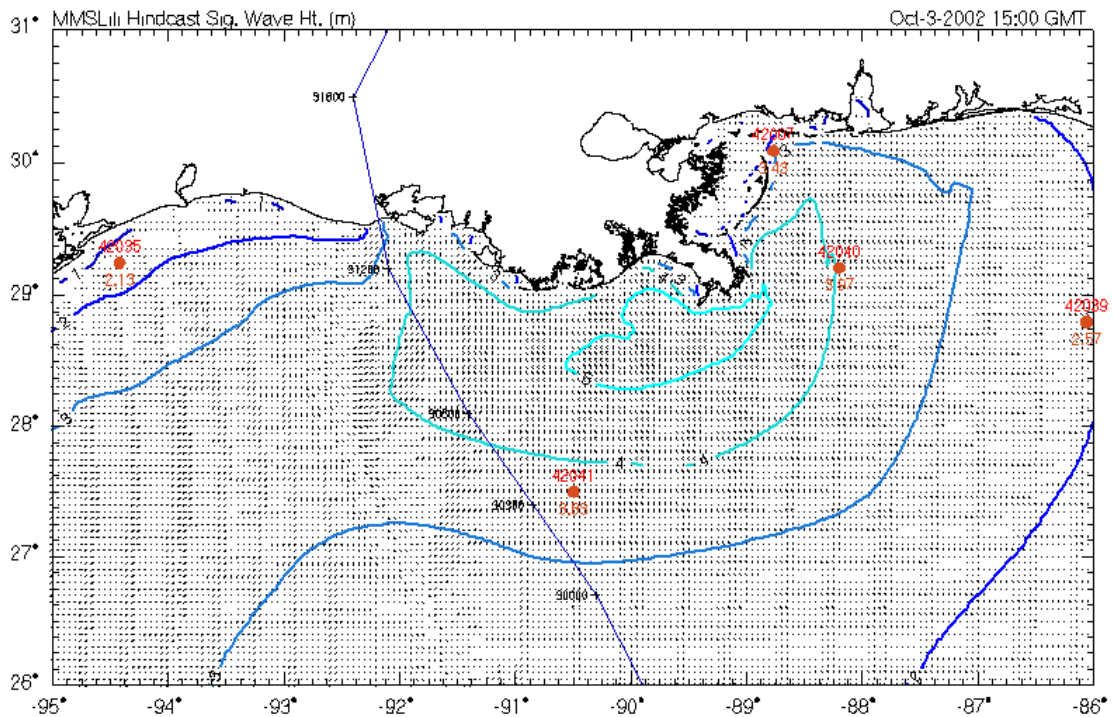
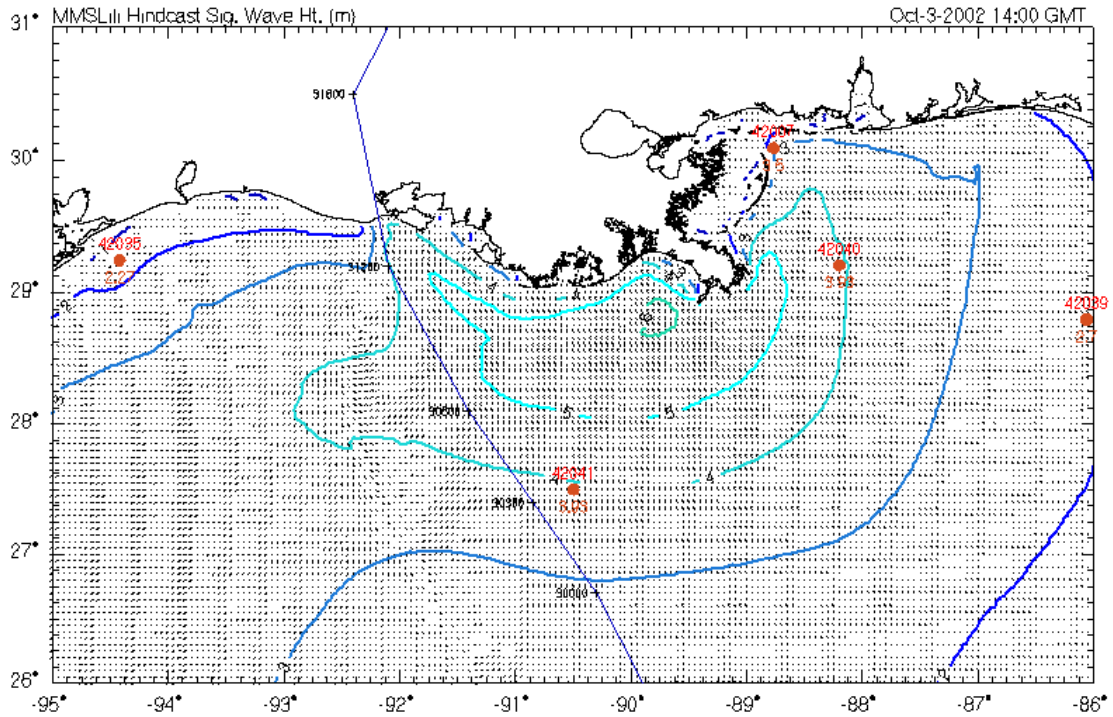












APPENDIX D. Fields Definitions

WD Wind Direction:

From which the wind is blowing, clockwise from true north in degrees (meteorological convention).

WS Wind Speed:

30-minute average of the effective neutral wind at a height of 10 meters, units in meters/second.

ETOT Total Variance of Total Spectrum:

The sum of the variance components of the hindcast spectrum, over the 552 bins of the 3G wave model, in meters squared.

TP Peak Spectral Period of Total Spectrum:

Peak period is the reciprocal of peak frequency, in seconds. Peak frequency is computed by taking the spectral density in each frequency bin, and fitting a parabola to the highest density and one neighbor on each side. If highest density is in the .32157 Hz bin, the peak period reported is the peak period of a Pierson-Moskowitz spectrum having the same total variance as the hindcast spectrum.

VMD Vector Mean Direction of Total Spectrum:

To which waves are traveling, clockwise from north in degrees (oceanographic convention).

Explanation of sea/swell computation:

The sum of the variance components of the hindcast spectrum, over the 552 bins of the 3G model, in meters squared. To partition sea (primary) and swell (secondary) we compute a P-M (Pierson-Moskowitz) spectrum, with a \cos^3 spreading, from the adopted wind speed and direction. For each of the 552 bins, the lesser of the hindcast variance component and P-M variance component is thrown into the sea partition; the excess, if any, of hindcast over P-M is thrown into the swell partition.

ETTSEA Total Variance of Primary Partition "Sea"

TPSEA Peak Spectral Period of Primary Partition:

VMDSEA Vector Mean Direction of Primary Partition:

ETTSW Total Variance of Secondary Partition: "Swell"

TPSW Peak Spectral Period of Secondary Partition:

VMDSW Vector Mean Direction of Secondary Partition:

MO1 First Spectral Moment of Total Spectrum:

Following Haring and Heideman (OTC 3280, 1978) the first and second moments contain powers of $\omega = 2\pi f$; thus:

$$M_1 = \sum \sum 2\pi f dS$$
$$M_2 = \sum \sum (2\pi f)^2 dS$$

where dS is a variance component and the double sum extend over 552 bins.

MO2 Second Spectral Moment of Total Spectrum:

HS Significant Wave Height:
4.000 times the square root of the total variance, in meters.

Dominant Direction: Following Haring and Heideman, the dominant direction ψ is the solution of the equations

$$A \cos 2\psi = \sum \sum \cos 2\theta \pi dS$$
$$A \sin 2\psi = \sum \sum \sin 2\theta \pi dS$$

The angle ψ is determined only to within 180 degrees. Haring and Heideman choose from the pair (ψ , $\psi+180$) the value closer to the peak direction.

Angular Spreading Function: The angular spreading function (Gumbel, Greenwood & Durand) is the mean value, over the 552 bins, of $\cos(\theta - \text{VMD})$, weighted by the variance component in each bin. If the angular spectrum is uniformly distributed over 360 degrees, this statistic is zero if uniformly distributed over 180 degrees, $2/\pi$ if all variance is concentrated at the VMD, 1. For the use of this statistic in fitting an exponential distribution to the angular spectrum, see Pearson & Hartley, Biometrika Tables for statisticians, 2:123 ff.

In-Line Variance Ratio: called directional spreading by Haring and Heideman, p 1542. Computed as:

$$Rat = \frac{\sum \sum \cos^2(\theta - \psi) dS}{\sum \sum dS}$$

If spectral variance is uniformly distributed over the entire compass, or over a semicircle, $Rat = 0.5$; if variance is confined to one angular band, or to two band 180 degrees apart, $Rat = 1.00$. According to Haring and Heideman, \cos^2 spreading corresponds to $Rat = 0.75$.